Trimers in the resonant (2 + 1)-fermion problem on a narrow Feshbach resonance: Crossover from Efimovian to hydrogenoid spectrum

Yvan Castin and Edoardo Tignone
Laboratoire Kastler Brossel, École Normale Supérieure and CNRS, UPMC, 24 rue Lhomond, F-75231 Paris, France
(Received 10 July 2011; published 8 December 2011)

We study the quantum three-body free-space problem of two same-spin-state fermions of mass m interacting with a different particle of mass M, on an infinitely narrow Feshbach resonance with infinite s-wave scattering length. This problem is made interesting by the existence of a tunable parameter, the mass ratio $\alpha = m/M$. By a combination of analytical and numerical techniques, we obtain a detailed picture of the spectrum of three-body bound states, within *each* sector of fixed total angular momentum l. For α increasing from 0, we find that the trimer states first appear at the l-dependent Efimovian threshold $\alpha_c^{(l)}$, where the Efimov exponent s vanishes, and that the *entire* trimer spectrum (starting from the ground trimer state) is geometric for α tending to $\alpha_c^{(l)}$ from above, with a global energy scale that has a finite and nonzero limit. For further increasing values of α, the least bound trimer states still form a geometric spectrum, with an energy ratio $\exp(2\pi/|s|)$ that becomes closer and closer to unity, but the most bound trimer states deviate more and more from that geometric spectrum and eventually form a hydrogenoid spectrum.

DOI: 10.1103/PhysRevA.84.062704 PACS number(s): 34.50.−s, 21.45.−v, 67.85.−d

I. INTRODUCTION

The quantum few-body problem is the subject of a renewed interest [1], thanks to the possibility of experimentally studying this problem in a resonant regime with cold atoms close to a Feshbach resonance [2]. In this resonant regime, the s-wave scattering length a associated to the interaction among the particles can be made much larger in absolute value than the interaction range. This has, in particular, allowed the physicists to study the Efimov effect in the laboratory, until now for three bosons and for three distinguishable particles [3], that is, the emergence for $1/a = 0$ of an infinite number of trimer states with an accumulation point at zero energy in the vicinity of which the spectrum forms a geometric sequence. Whereas the existence of an infinite number of bound states is common for long-range interactions (vanishing for diverging interparticle distance r_{12} as $1/r_{12}^2$ or more slowly), this is quite intriguing for short-range interactions. Initially predicted by Efimov for three bosons, this effect can actually take place in more general situations [4], in particular, in the so-called (2 + 1)-fermion problem if the extra particle is light enough [5].

What we call here the (2 + 1)-fermion problem consists in the system of two same-spin-state fermions of mass m interacting with a particle of mass M of another species. It is assumed that there is no direct interaction among the fermions, whereas there is a resonant interaction between each fermion and the extra particle, that is, with an infinite s-wave scattering length, $1/a = 0$. Furthermore, it is assumed that this resonant interaction is due to an infinitely narrow Feshbach resonance, that is, of vanishing van der Waals range $b \to 0$ and finite effective range r_e.

This concept is most easily understood in a two-channel model. In the open channel, the particles exist in the form of atoms, and have a weak, nonresonant direct van der Waals interaction corresponding to the background scattering length $a_{\rm bg} \approx b$ and the interaction range b. In the closed channel, the particles exist in the form of a bound state of a fermion with the other-species atom, the so-called closed-channel molecule with radius $\approx b$. Due to a coupling Λ between the two channels, which we shall define precisely later, the closed-channel molecule is coherently converted into a pair of atoms in the open channel, and vice versa. For an appropriate Zeeman tuning (with a magnetic field) of the bare energy $E_{\rm mol}$ of the closed-channel molecule with respect to the dissociation limit of the open channel, the s-wave scattering length a between a fermion and the other-species atom is infinite. In this case, in simple models, the effective range r_e is the sum of two contributions [6]. The first one is, as expected, of the order of the van der Waals length b. The second one is induced by the interchannel coupling; it is expressed as $-2R_*$ [7], where the Feshbach length R_* is positive and scales as $1/\Lambda^2$:

$$R_* = \frac{\pi\hbar^4}{\Lambda^2\mu^2}, \tag{1}$$

where μ is the reduced mass of a fermion and the other-species particle. When the interchannel coupling Λ is very weak, this second contribution dominates over the first one, $R_* \gg b$, and this is the narrow Feshbach resonance regime. An example under current theoretical and experimental investigation is the case of the interspecies Feshbach resonances of the fermionic ^{6}Li and the fermionic ^{40}K, which are narrow: The Feshbach length R_* exceeds 100 nm, whereas the van der Waals length is a few nanometers [8–10].

To obtain the infinitely narrow Feshbach resonance model, here for $1/a = 0$, one takes the mathematical limit of a vanishing van der Waals range b with a fixed nonzero interchannel coupling Λ. The s-wave scattering amplitude between one fermion and the extra particle for a relative wave vector $\mathbf{k}$ is then [7]

$$f_k = \frac{-1}{ik + k^2 R_*}. \tag{2}$$

This implies the absence of two-body bound states, since f_k cannot have a pole for $k = iq, q > 0$. The model can, however, certainly support trimer states since the (2 + 1)-fermion problem is subjected to the Efimov effect for a large-enough mass ratio m/M [4,5].

The main motivation of the present work is to study the spectrum of trimers for this problem in free space for $1/a = 0$, in particular, to determine analytically the global energy scale of the Efimovian part of the spectrum, related to the so-called three-body parameter. This global energy scale is out of reach of Efimov's zero-range theory [4] but it was determined analytically for three bosons for a narrow Feshbach resonance in Refs. [11,12]. Here we shall generalize this calculation to the present (2 + 1)-fermion problem. A second motivation is to determine the low-lying states of each Efimov trimer series, which, in principle, are not accurately described by Efimov theory, and to look for possible trimer states that are not related to the Efimov effect and may, thus, appear for lower mass ratios.

The paper is organized as follows. After a presentation of the model and the derivation of an integral equation *à la* Skorniakov-Ter-Martirosian [13] for the three-body problem in momentum space in Sec. II, analytical solutions of this integral equation are obtained in limiting cases in Sec. III. In the Sec. IV, we analytically explore the physics of the trimers; of particular interest are the exact results on the global energy scale in the Efimovian part of the spectrum, see Sec. IV B, and the study of an hydrogenoid part of the spectrum in the Born-Oppenheimer regime, see Sec. IV C. An efficient numerical solution of the integral equation is used in Sec. V to explore intermediate regimes not covered by the analytics. We conclude in Sec. VI.

II. THE MODEL AND THE GENERAL MOMENTUM SPACE EQUATION

A tractable though realistic description of a Feshbach resonance is obtained with the so-called two-channel models, where the particles exist either in the form of atoms in the open channel or in the form of molecules in the closed channel [2,14–20]. We use here the same free-space two-channel model Hamiltonian H as in Ref. [21] written in momentum space in second quantized form in terms of the fermionic annihilation operators $c_{\mathbf{k}}$, the extra-particle annihilation operators $a_{\mathbf{k}}$ and the closed-channel molecule annihilation operators $b_{\mathbf{k}}$:

$$H = H_{\rm at} + H_{\rm mol} + H_{\rm at-mol} + H_{\rm open}, \tag{3}$$

with

$$H_{\rm at} = \int \frac{d^3k}{(2\pi)^3}[E_{\mathbf{k}} c^\dagger_{\mathbf{k}} c_{\mathbf{k}} + \alpha E_{\mathbf{k}} a^\dagger_{\mathbf{k}} a_{\mathbf{k}}], \tag{4}$$

$$H_{\rm mol} = \int \frac{d^3k}{(2\pi)^3}\left(E_{\rm mol} + \frac{\alpha}{1+\alpha}E_{\mathbf{k}}\right) b^\dagger_{\mathbf{k}} b_{\mathbf{k}}, \tag{5}$$

$$H_{\rm at-mol} = \Lambda \int \frac{d^3k_1 d^3k_2}{[(2\pi)^3]^2}\chi(\mathbf{k}_{12})\left[b^\dagger_{\mathbf{k}_1+\mathbf{k}_2} a_{\mathbf{k}_1} c_{\mathbf{k}_2} + \text{H.c.}\right], \tag{6}$$

$$H_{\rm open} = g_0 \int \frac{d^3k_1 d^3k_2 d^3k_3 d^3k_4}{[(2\pi)^3]^4}\chi(\mathbf{k}_{12})\chi(\mathbf{k}_{43}) \times (2\pi)^3\delta(\mathbf{k}_1+\mathbf{k}_2-\mathbf{k}_3-\mathbf{k}_4) a^\dagger_{\mathbf{k}_4} c^\dagger_{\mathbf{k}_3} c_{\mathbf{k}_2} a_{\mathbf{k}_1}. \tag{7}$$

Whereas the $c_{\mathbf{k}}$ obey the usual free-space anticommutation relations

$$\{c_{\mathbf{k}}, c^\dagger_{\mathbf{k}'}\} = (2\pi)^3\delta(\mathbf{k}-\mathbf{k}'), \tag{8}$$

the statistical nature (fermionic or bosonic) of the extra particle and of the closed-channel molecule does not need to be specified here, since there will be at most one of the particles in the state vector. Simply, the $c_{\mathbf{k}}$ and $c^\dagger_{\mathbf{k}}$ commute with $a_{\mathbf{k}}$ and $b_{\mathbf{k}}$. In the kinetic energy terms of the atoms $H_{\rm at}$ and of the closed-channel molecule $H_{\rm mol}$, we have introduced the free fermion dispersion relation $E_{\mathbf{k}} = \hbar^2k^2/(2m)$ and the mass ratio of a fermion to the extra particle:

$$\alpha \equiv \frac{m}{M}. \tag{9}$$

The internal energy $E_{\rm mol}$ of the closed-channel molecule is counted with respect to the dissociation limit of the open channel and is experimentally adjusted thanks to the Zeeman effect by tuning of the external magnetic field. $H_{\rm at-mol}$ represents the coherent interconversion of a closed-channel molecule into one fermionic atom and the extra particle, due to the coupling between the closed channel and the open channel. It involves the interchannel coupling constant Λ and is regularized by the momentum space cutoff function χ, assumed to be real and rotationally invariant, that tends to 1 at zero momentum and that rapidly tends to zero at large momenta with a width $1/b$, where the interaction range b is of the order of the van der Waals length. Note that the argument of the cut-off function χ is the relative wave vector of a fermion (of momentum $\hbar\mathbf{k}_2$) with respect to the extra particle (of momentum $\hbar\mathbf{k}_1$):

$$\mathbf{k}_{12} \equiv \mu\left(\frac{\mathbf{k}_2}{m} - \frac{\mathbf{k}_1}{M}\right) = \frac{\mathbf{k}_2 - \alpha\mathbf{k}_1}{1+\alpha}, \tag{10}$$

where

$$\mu = \frac{mM}{m+M} \tag{11}$$

is the reduced mass to preserve Galilean invariance. Finally, $H_{\rm open}$ models the direct interaction between atoms in the open channel, in the form of a separable potential with bare coupling constant g_0 and the same cut-off function χ as in $H_{\rm at-mol}$. This direct interaction is characterized by the so-called background scattering length $a_{\rm bg}$. The inclusion of both $H_{\rm at-mol}$ and $H_{\rm open}$ allows us to recover the usual expression for the scattering length as a function of the magnetic field B [2],

$$a(B) = a_{\rm bg}\left(1 - \frac{\Delta B}{B - B_0}\right), \tag{12}$$

if $E_{\rm mol}$ is taken to be an affine function of B. The quantity ΔB is the so-called magnetic width of the Feshbach resonance.

We now derive from the model Hamiltonian a momentum space integral equation *à la* Skorniakov-Ter-Martirosian [13] for the three-body problem of two fermions and one extra particle, closely following Ref. [21] downgraded from the 3 + 1 to the 2 + 1 case. In the search for bound states, we take a negative eigenenergy, $E < 0$, and we express Schrödinger's equation $0 = (H - E)|\Psi\rangle$ for a ket of zero total momentum and being the sum of general ansatz with zero or one closed-channel molecule, $|\Psi\rangle = |\psi_{3\,\text{at}}\rangle + |\psi_{1\,\text{at}+1\,\text{mol}}\rangle$, with

$$|\psi_{3\,\text{at}}\rangle = \int \frac{d^3k_1 d^3k_2 d^3k_3}{[(2\pi)^3]^3}(2\pi)^3\delta(\mathbf{k}_1+\mathbf{k}_2+\mathbf{k}_3) \times A(\mathbf{k}_1,\mathbf{k}_2,\mathbf{k}_3) a^\dagger_{\mathbf{k}_1} c^\dagger_{\mathbf{k}_2} c^\dagger_{\mathbf{k}_3}|0\rangle,$$
$$|\psi_{1\,\text{at}+1\,\text{mol}}\rangle = \int \frac{d^3k}{(2\pi)^3} B(\mathbf{k}) b^\dagger_{-\mathbf{k}} c^\dagger_{\mathbf{k}}|0\rangle. \tag{13}$$

Thanks to the fermionic antisymmetry we can impose that $A(\mathbf{k}_1,\mathbf{k}_2,\mathbf{k}_3)$ is an antisymmetric function of $\mathbf{k}_2$ and $\mathbf{k}_3$. On the contrary, a fermionic atom and a closed-channel molecule are distinguishable objects and there is no exchange symmetry constraint on the function $B(\mathbf{k})$. Projecting Schrödinger's equation on the subspace with three atoms, and using $E < 0$, we are able to express A in terms of B and of an auxiliary unknown function $\tilde{B}$ obtained by a partial contraction of A:

$$\tilde{B}(\mathbf{k}_3) = \int \frac{d^3k_1 d^3k_2}{[(2\pi)^3]^2}\chi(\mathbf{k}_{12})(2\pi)^3\delta(\mathbf{k}_1+\mathbf{k}_2+\mathbf{k}_3)A(\mathbf{k}_1,\mathbf{k}_2,\mathbf{k}_3).$$

More precisely,

$$A(\mathbf{k}_1,\mathbf{k}_2,\mathbf{k}_3) = \frac{\Lambda/2}{E-(\alpha E_{\mathbf{k}_1}+E_{\mathbf{k}_2}+E_{\mathbf{k}_3})} \times [\chi(\mathbf{k}_{12})D(\mathbf{k}_3) - \chi(\mathbf{k}_{13})D(\mathbf{k}_2)], \tag{14}$$

where the convenient unknown function is actually D such that

$$\Lambda D(\mathbf{k}) = \Lambda B(\mathbf{k}) + 2g_0\tilde{B}(\mathbf{k}). \tag{15}$$

Plugging the expression (14) of A into the definition of $\tilde{B}$ gives the first important equation,

$$\frac{2}{\Lambda}\tilde{B}(\mathbf{k}_3) = \int \frac{d^3k_1 d^3k_2}{[(2\pi)^3]^2}\chi(\mathbf{k}_{12})\frac{(2\pi)^3\delta(\mathbf{k}_1+\mathbf{k}_2+\mathbf{k}_3)}{E-(\alpha E_{\mathbf{k}_1}+E_{\mathbf{k}_2}+E_{\mathbf{k}_3})} \times [\chi(\mathbf{k}_{12})D(\mathbf{k}_3) - \chi(\mathbf{k}_{13})D(\mathbf{k}_2)]. \tag{16}$$

The second important equation is obtained by projecting Schrödinger's equation on the subspace with one atom and one closed-channel molecule (in which case the direct open-channel interaction cannot contribute):

$$2\Lambda\tilde{B}(\mathbf{k}) = [E_{\text{rel}}(\mathbf{k}) - E_{\text{mol}}]B(\mathbf{k}), \tag{17}$$

where we have introduced what we call the relative energy

$$E_{\text{rel}}(\mathbf{k}) = E - \left(E_{\mathbf{k}} + \frac{\alpha}{1+\alpha}E_{\mathbf{k}}\right). \tag{18}$$

This is indeed the relative energy of one of the fermions and of the extra particle, knowing that the second fermion has a wave vector $\mathbf{k}$, since one subtracts in Eq. (18) from the total energy E the kinetic energy $E_{\mathbf{k}}$ of the second fermion and the center-of-mass kinetic energy of the first-fermion-plus-extra-particle. One expresses $\tilde{B}$ in terms of D by elimination of B between (15) and (17). One then eliminates $\tilde{B}$ between the resulting equation and (16) to finally obtain a closed equation for D as follows:

$$0 = \frac{\mu D(\mathbf{k}_3)}{2\pi\hbar^2 f[E_{\text{rel}}(\mathbf{k}_3)]} - \int \frac{d^3k_1 d^3k_2}{[(2\pi)^3]^2}(2\pi)^3\delta(\mathbf{k}_1+\mathbf{k}_2+\mathbf{k}_3) \times \frac{\chi(\mathbf{k}_{12})\chi(\mathbf{k}_{13})D(\mathbf{k}_2)}{E-(\alpha E_{\mathbf{k}_1}+E_{\mathbf{k}_2}+E_{\mathbf{k}_3})}. \tag{19}$$

The function f is related to the two-body T matrix for the scattering of a fermion and of the extra particle [21],

$$\langle\mathbf{k}_f|T(\epsilon+i0^+)|\mathbf{k}_i\rangle = -\frac{2\pi\hbar^2}{\mu}\chi(\mathbf{k}_f)\chi(\mathbf{k}_i)f(\epsilon+i0^+), \tag{20}$$

where the relative wave vectors $\mathbf{k}_i$, $\mathbf{k}_f$ and the energy ϵ are arbitrary (the T matrix is not necessarily on shell in that expression).

The general expression of f is given in Ref. [21]. Here, however, we shall concentrate on the limit of an infinitely narrow Feshbach resonance. We thus take the zero-range limit $b \to 0$, in which case the cut-off function χ (of width $\propto 1/b$) tends to unity. It is assumed that there is no resonant interaction in the open channel, so the corresponding background scattering length a_{bg} is $O(b)$ and also tends to zero. On the contrary, the interchannel coupling Λ is kept fixed to keep a nonzero effective range, and E_{mol} is adjusted to keep a fixed value of the scattering length a. In this case, the function f for a positive and fixed energy $\epsilon > 0$ (so $\mu b^2\epsilon/\hbar^2 \to 0$) simply tends to the s-wave scattering amplitude f_k on an infinitely narrow Feshbach resonance [7]:

$$f(\epsilon+i0^+) = f_k \tag{21}$$

with

$$f_k = -\frac{1}{a^{-1}+ik+k^2R_*}. \tag{22}$$

The Feshbach length R_* is expressed in terms of the width ΔB of the Feshbach resonance as [7]

$$R_* = \frac{\hbar^2}{2\mu a_{\text{bg}}\mu_b\Delta B}, \tag{23}$$

where the differential magnetic moment between the closed and open channels is $\mu_b = dE_{\text{mol}}/dB$ taken for $B = B_0$. In Eq. (22), the relative wavenumber $k = (2\mu\epsilon)^{1/2}/\hbar$ since the energy is positive. For a negative energy, the function f has the same expression (21) if one uses the analytic continuation $k = i(-2\mu\epsilon)^{1/2}/\hbar$ in f_k [22].

It is convenient to represent the eigenenergy E in terms of a wave number, setting

$$E = -\frac{\hbar^2q^2}{2\mu}, \tag{24}$$

where we recall that $\mu = mM/(m+M)$ is the reduced mass and $q \geqslant 0$. Similarly, the relative energy is represented by a wave number, $E_{\text{rel}}(\mathbf{k}) = -\hbar^2q^2_{\text{rel}}(k)/(2\mu)$ leading to

$$q_{\text{rel}}(k) = \left[q^2 + \frac{1+2\alpha}{(1+\alpha)^2}k^2\right]^{1/2}. \tag{25}$$

For an infinitely narrow s-wave Feshbach resonance with a scattering length a, the integral equation resulting from Schrödinger's equation, the equivalent of the Skorniakov-Ter-Martirosian equation [13] for our problem, is then

$$0 = \left[-a^{-1} + q_{\text{rel}}(k) + q^2_{\text{rel}}(k)R_*\right]D(\mathbf{k}) + \int \frac{d^3k'}{2\pi^2}\frac{D(\mathbf{k}')}{q^2+k^2+k'^2+\frac{2\alpha}{1+\alpha}\mathbf{k}\cdot\mathbf{k}'}. \tag{26}$$

In that equation, for the sake of generality, we have kept an arbitrary value of the scattering length a. In what follows, we shall restrict our study to the exact resonance location where $1/a = 0$.

We shall also take advantage of rotational invariance to reduce the integral equation to an unknown function of a single variable only, as done in Ref. [13]. The eigenstates of the Hamiltonian H may be assumed of a fixed total angular momentum of angular quantum number l. Without loss of generality one can also assume that the angular momentum along the quantization axis z is zero. The corresponding ansatz for D is, thus,

$$D(\mathbf{k}) = Y_l^0(\mathbf{k}) f^{(l)}(k), \tag{27}$$

where the notation $Y_l^{m_l}(\mathbf{k})$ stands for the spherical harmonics $Y_l^{m_l}(\theta,\phi)$, where θ and ϕ are, respectively, the polar and azimuthal angles of the vector $\mathbf{k}$ in a system of spherical coordinates of polar axis z. The unknown function $f^{(l)}$ then depends only on the modulus k of $\mathbf{k}$. We see that this also fixes the parity of the eigenstate to the value $(-1)^l$. In the integral over $\mathbf{k}'$ in Eq. (26), we then perform the change of variable of unit Jacobian,

$$\mathbf{k}' = \mathcal{R}\mathbf{K}, \tag{28}$$

where $\mathcal{R}$ is the rotation in $\mathbb{R}^3$ defined by the Euler decomposition of its inverse:

$$\mathcal{R}^{-1} = \mathcal{R}_z(-\phi)\mathcal{R}_y(\theta)\mathcal{R}_z(\pi - \phi), \tag{29}$$

where the notation $\mathcal{R}_i(\alpha)$ stands for the rotation of an angle α around the axis $i \in \{x,y,z\}$. This choice ensures that $\mathbf{k}/k = \mathcal{R}\mathbf{e}_z$, where $\mathbf{e}_z$ is the unit vector defining the z axis. In the denominator of the integrand of (26), the scalar product $\mathbf{k}\cdot\mathbf{k}'$ is then transformed as $k\mathbf{e}_z \cdot \mathbf{K}$, so the denominator is invariant by rotation of $\mathbf{K}$ around z. In the numerator we use the transformation of spherical harmonics under rotation, see Eqs. (8.6-2) and (8.6-1) in Ref. [23], and the relation $[Y_l^{m_l}(\theta,-\phi)]^* = Y_l^{m_l}(\theta,\phi)$:

$$Y_l^0(\mathcal{R}\mathbf{K}) = \left(\frac{4\pi}{2l+1}\right)^{1/2} \sum_{m_l=-l}^{l} Y_l^{m_l}(\mathbf{k}) Y_l^{m_l}(\mathbf{K}), \tag{30}$$

which, in particular, allows us to pull out the factors $Y_l^{m_l}(\mathbf{k})$ expected from rotational invariance. The integration over $\mathbf{K}$ is then conveniently performed in spherical coordinates of polar axis z. All the terms with $m_l \neq 0$ in Eq. (30) vanish in the integration over the azimuthal angle of $\mathbf{K}$. From the expression of the spherical harmonics in terms of the Legendre polynomial of degree l [23],

$$Y_l^0(\mathbf{K}) = \left(\frac{4\pi}{2l+1}\right)^{-1/2} P_l(u = \mathbf{K}\cdot\mathbf{e}_z/K), \tag{31}$$

we finally obtain the reduced integral equation to be solved in the sector of angular momentum l, for $1/a = 0$:

$$0 = \left[q_{\rm rel}(k) + q_{\rm rel}^2(k)R_*\right] f^{(l)}(k) + \int_0^{+\infty} \frac{dK}{\pi} f^{(l)}(K) \int_{-1}^{1} du\, \frac{P_l(u)K^2}{q^2 + k^2 + K^2 + \frac{2\alpha}{1+\alpha} kKu}. \tag{32}$$

III. ANALYTICAL SOLUTIONS IN PARTICULAR CASES

Several remarkable analytical techniques are now available to solve the three-body problem in some appropriate limiting cases [5,11,12,24,25]. Whereas we do not know how to solve Eq. (32) analytically in general, it is possible to find solutions when there is an extra symmetry available, that is, scale invariance. The most standard regime corresponds to the limit $R_* \to 0$, in which case our model reduces to the so-called zero-range or Bethe-Peierls model, where the interactions are included via two-body contact conditions on the wave function [26]. Since $1/a = 0$, these contact conditions are indeed scaling invariant, which allows us to fully solve the problem [4,27]. Because the zero-range model is usually solved in position space, it is interesting here to briefly show the calculations in momentum space. In the regime of interest, where the Efimov effect takes place, the zero-range model is, however, not well defined, and an extra three-body condition has to be introduced to make it self-adjoint [28], involving the three-body parameter.

The relevant case here, therefore, is $R_* > 0$. The existence of such a finite-length scale characterizing the interactions breaks the scale invariance. Fortunately, as shown in Ref. [12], if one restricts the study to the zero-energy case $E = 0$, equations such as Eq. (32) can still be solved analytically. This gives access to the three-body parameter, and, thus, to the characterization of the Efimov spectrum of trimers.

A. Zero-range case ($R_* = 0$) at zero energy

For $R_* = 0$ and at zero energy $q = 0$, the integral Eq. (32) is manifestly scaling invariant: If $f^{(l)}(k)$ is a solution, the function $f_\lambda^{(l)}(k) = f^{(l)}(k/\lambda)$ is also a solution, $\forall\lambda > 0$, and we expect that the two functions $f^{(l)}$ and $f_\lambda^{(l)}$ are proportional. We thus seek a solution in the form of a power law,

$$f^{(l)}(k) = k^{-(s+2)}. \tag{33}$$

The form of the exponent results from the general theory (see section 3.3 in Ref. [29]): For an N-body problem (here $N = 3$) and for s to be a direct generalization of the exponent s_0 introduced by Efimov [4], the exponent in Eq. (33) should be $-[s + (3N-5)/2]$. For convergence issues, it is simpler to assume in explicit calculations that $s = iS$, where S is real. By analytic continuation, the result, however, also extends to real s, as also shown by the real-space calculation [30]. We inject the ansatz [Eq. (33)] in Eq. (32) with $q = 0$, $R_* = 0$, and we perform the change of variable $K = ke^x$ to obtain an equation for s,

$$0 = \Lambda_l(s), \tag{34}$$

with the function

$$\Lambda_l(s) \equiv \frac{(1+2\alpha)^{1/2}}{1+\alpha} + \int_{-1}^{1} du\, P_l(u) \int_{-\infty}^{+\infty} \frac{dx}{2\pi} \frac{e^{-iSx}}{\cosh x + \frac{\alpha}{1+\alpha}u}. \tag{35}$$

Using contour integration and the Cauchy residue formula, the integral over x may be calculated: Setting $\theta = \arccos\left(\frac{\alpha}{1+\alpha}u\right)$, so $\theta \in [0,\pi]$, we obtain

$$\int_{-\infty}^{+\infty} \frac{dx}{2\pi} \frac{e^{-iSx}}{\cosh x + \frac{\alpha}{1+\alpha}u} = \frac{\sin(s\theta)}{\sin(s\pi)\sin\theta}. \quad (36)$$

Successive integration over u is simplified by taking θ rather than u as integration variable, with a Jacobian that simplifies with the factor $\sin\theta$ in the denominator of Eq. (36). Following [5] we then parametrize the mass ratio by an angle $\nu \in]0,\pi/2[$:

$$\nu = \arcsin\frac{\alpha}{1+\alpha} = \arcsin\frac{m}{m+M}, \quad (37)$$

which leads to the remarkable property

$$\cos\nu = \frac{(1+2\alpha)^{1/2}}{1+\alpha}. \quad (38)$$

Also using $\arccos[\alpha/(1+\alpha)] = \frac{\pi}{2} - \nu$, we obtain

$$\Lambda_l(s) = \cos\nu + \frac{1}{\sin\nu}\int_{\frac{\pi}{2}-\nu}^{\frac{\pi}{2}+\nu} d\theta\, P_l\left(\frac{\cos\theta}{\sin\nu}\right)\frac{\sin(s\theta)}{\sin(s\pi)}. \quad (39)$$

This can be further simplified, taking advantage of the parity of the Legendre polynomial, $P_l(-u) = (-1)^l P_l(u)$, for all u by shifting the integration variable θ by $\pi/2$. Depending on the even or odd parity of the angular momentum l this reduces to

$$\Lambda_l(s) \overset{l\,\text{even}}{=} \cos\nu + \frac{1}{\sin\nu}\int_0^{\nu} d\theta\, P_l\left(\frac{\sin\theta}{\sin\nu}\right)\frac{\cos(s\theta)}{\cos(s\pi/2)}, \quad (40)$$

$$\Lambda_l(s) \overset{l\,\text{odd}}{=} \cos\nu - \frac{1}{\sin\nu}\int_0^{\nu} d\theta\, P_l\left(\frac{\sin\theta}{\sin\nu}\right)\frac{\sin(s\theta)}{\sin(s\pi/2)}. \quad (41)$$

Equation (41) will be quite useful to obtain analytical results on the Efimovian trimer spectrum in the large α limit; see Secs. IV A and IV B.

An explicit expression of $\Lambda_l(s)$ as a sum of a finite number of simple functions of s may be obtained by representing the function $P_l\left(\frac{\sin\theta}{\sin\nu}\right)$ as a Fourier sum, that is, a sum of $\cos n\theta$, $0 \leqslant n \leqslant l$, n even, for an even l and a sum of $\sin n\theta$, $1 \leqslant n \leqslant l$, n odd, for an odd l. The coefficients are polynomials of $1/\sin\nu$ that are simple to calculate analytically from the known coefficients of the Legendre polynomials $P_l(u)$ [31]. The resulting integrals over θ, e.g., of $\sin(n\theta)\sin(s\theta)$, are then straightforward to evaluate. We finally obtain the explicit formula valid for arbitrary parity of l:

$$\Lambda_l(s) = \cos\nu + \frac{1}{\sin\nu\cos[(s+l)\pi/2]} \times \sum_{n=0}^{l} c_n \left\{\frac{\sin[(s+n)\nu]}{s+n} + (-1)^l \frac{\sin[(s-n)\nu]}{s-n}\right\}. \quad (42)$$

The coefficients c_n are zero for $l-n$ odd. For $l-n$ even,

$$c_n = \left(1 - \frac{1}{2}\delta_{n,0}\right)\frac{(-1)^{(l+n)/2}}{(4\sin\nu)^l} \times \sum_{k=0}^{(l-n)/2} \frac{(-4\sin^2\nu)^k(2l-2k)!}{k!(l-k)!\left(\frac{l-n}{2}-k\right)!\left(\frac{l+n}{2}-k\right)!}, \quad (43)$$

where δ_{ij} is the usual Kronecker δ.

Equation (42) has the interesting feature that the coefficients are s independent, which makes the numerical evaluation of $\Lambda_l(s)$ as a function of s particularly efficient. As a test, it is, however, interesting to compare to the transcendental equation for s obtained by the direct calculation *à la* Efimov in position space. As detailed in Appendix A, introducing the hypergeometric function ${}_2F_1$ as in Ref. [32] to solve some differential equation, we generalize the formulas of Ref. [32] to an arbitrary mass ratio, a generalization that was done with the adiabatic hyperspherical method in Ref. [33]:

$$\Lambda_l(s) = \cos\nu + (-1)^l \sin^l\nu\, \frac{\Gamma(\frac{l+1+s}{2})\Gamma(\frac{l+1-s}{2})}{2\pi^{1/2}\Gamma(l+\frac{3}{2})} \times {}_2F_1\left(\frac{l+1+s}{2}, \frac{l+1-s}{2}, l+\frac{3}{2}; \sin^2\nu\right), \quad (44)$$

where Γ is the Γ function. A variant of Eq. (44) will be quite useful to obtain analytical results on the Efimovian trimer spectrum in the large l limit; see Secs. IV A and IV B.

B. Zero-range case ($R_* = 0$) at negative energy

Once the imaginary values of the Efimov exponent s are determined by solution of the transcendental equation $\Lambda_l(s) = 0$, which is possible for l odd and α larger than a critical value $\alpha_c^{(l)}$, see Sec. IV A, one can determine the corresponding Efimovian trimer solutions of the zero-range theory at arbitrary energies, in free space and also in an isotropic harmonic trap, using the general real-space formalism relying on separability of the Bethe-Peierls problem in hyperspherical coordinates [27,29,30]. Here we find it interesting to deduce from the real-space solution the explicit form of the momentum-space solution, restricting for simplicity to the values of the mass ratio α and the (necessarily odd) angular momentum l such that the Efimov effect takes place. This may be useful, for example, to calculate the atomic momentum distribution of the Efimov trimer states in the zero-range limit, as was done for three bosons in Ref. [34].

The idea to obtain $D(\mathbf{k})$ is to take the limit of the position $\mathbf{r}_1$ of the extra particle and the position $\mathbf{r}_2$ of a fermionic atom converging to the same location, with a fixed value of their center-of-mass position and of the position $\mathbf{r}_3$ of the second fermionic atom. According to the Bethe-Peierls framework, the atomic wave function $\psi(\mathbf{r}_1,\mathbf{r}_2,\mathbf{r}_3)$ shall then diverge as $1/r$, with $\mathbf{r} = \mathbf{r}_1 - \mathbf{r}_2$, with a factor depending on the Jacobi coordinate $\mathbf{x} = \mathbf{r}_3 - (M\mathbf{r}_1 + m\mathbf{r}_2)/(M+m)$:

$$\psi(\mathbf{r}_1,\mathbf{r}_2,\mathbf{r}_3) \underset{r\to 0}{\overset{\mathbf{x}\text{ fixed}}{\sim}} \frac{\mathcal{A}(\mathbf{x})}{r}. \quad (45)$$

One then calculates $\mathcal{A}(\mathbf{x})$ in two different ways. First, one uses the Efimov solution discussed in Appendix A: From Efimov's ansatz [Eq. (A1)] and from the solution $F(R) \propto K_s[(\bar{m}/\mu)^{1/2}qR]$ of the hyper-radial Eq. (A6), where $\bar{m}$ is an arbitrary mass unit and K_s a Bessel function, one finds for a vanishing angular momentum along z,

$$\mathcal{A}(\mathbf{x}) \propto Y_l^0(\mathbf{x})\frac{K_s(Qx)}{x}, \tag{46}$$

where we have set

$$Q \equiv q\left(\frac{\mu_{\rm am}}{\mu}\right)^{1/2} = \frac{1+\alpha}{(1+2\alpha)^{1/2}}q = \frac{q}{\cos\nu}, \tag{47}$$

where $\mu_{\rm am}$ is the reduced mass of one fermionic atom of mass m and one pair of fermion-plus-extra-particle of mass $m+M$. Second, after inspection of Eq. (13), one calculates the atomic wave function ψ by taking the Fourier transform of $A(\mathbf{k}_1,\mathbf{k}_2,\mathbf{k}_3)(2\pi)^3\delta(\mathbf{k}_1+\mathbf{k}_2+\mathbf{k}_3)$, where A is given by Eq. (14), taking the functions χ equal to unity. As expected, the contribution involving $\chi(\mathbf{k}_{12})D(\mathbf{k}_3)$ is the one leading to a divergence of ψ for $r\to 0$. Integration over $\mathbf{k}_1$ is straightforward thanks to the factor $(2\pi)^3\delta(\mathbf{k}_1+\mathbf{k}_2+\mathbf{k}_3)$. Integration over $\mathbf{k}_2$ then can be done after the change of variable $\mathbf{k}_2=\mathbf{k}_2'-\frac{\alpha}{1+\alpha}\mathbf{k}_3$ by use of

$$\int \frac{d^3k_2'}{(2\pi)^3}\frac{e^{-i\mathbf{k}_2'\cdot\mathbf{r}}}{k_2'^2+K^2} = \frac{e^{-Kr}}{4\pi r}, \tag{48}$$

where $K=[q^2+\frac{1+2\alpha}{(1+\alpha)^2}k_3^2]^{1/2}>0$. For $r\to 0$, one approximates e^{-Kr}/r with $1/r$ and one obtains

$$\mathcal{A}(\mathbf{x}) \propto \int \frac{d^3k_3}{(2\pi)^3}D(\mathbf{k}_3)e^{i\mathbf{k}_3\cdot\mathbf{x}}. \tag{49}$$

We thus set, for an arbitrary choice of normalization leading to a dimensionless function,

$$D(\mathbf{k}) = \int d^3x\, e^{-i\mathbf{k}\cdot\mathbf{x}}Y_l^0(\mathbf{x})\frac{Q^2K_s(Qx)}{x}. \tag{50}$$

A first technique to calculate the integral in Eq. (50) is to use the expansion of the plane wave on spherical harmonics: According to the identity (8.7-13) in Ref. [23], the amplitude of the function $\mathbf{x}\to e^{i\mathbf{k}\cdot\mathbf{x}}$ on the spherical harmonics $Y_l^{m_l}(\mathbf{x})$ is $4\pi i^l j_l(kx)[Y_l^{m_l}(\mathbf{k})]^*$, where the spherical Bessel function is real and may be expressed in terms of the usual Bessel function J:

$$j_l(kr) = \left(\frac{\pi}{2kr}\right)^{1/2}J_{l+1/2}(kr). \tag{51}$$

It turns out that the integral over $\mathbb{R}^+$ of the product of a power law and of two Bessel functions may be expressed exactly in terms of the hypergeometric function ${}_2F_1$, see relation 6.576(3) in Ref. [31]:

$$D(\mathbf{k}) = 2\pi^{3/2}(-i)^l(k/Q)^lY_l^0(\mathbf{k})\frac{\left|\Gamma\left(1+\frac{l+s}{2}\right)\right|^2}{\Gamma(l+3/2)} \times {}_2F_1\left(1+\frac{l+s}{2},1+\frac{l-s}{2},l+\frac{3}{2};-k^2/Q^2\right). \tag{52}$$

This immediately shows that $D(\mathbf{k})$ vanishes as k^l for $k\to 0$, which is generically the case for a regular function of angular momentum l. It also allows us to obtain the large momentum behavior of $D(\mathbf{k})$ [35],

$$D(\mathbf{k}) \underset{k/Q\to+\infty}{=} \frac{i\pi^2Q^2}{k^2\cos(\pi s/2)}Y_l^0(\mathbf{k})\left\{\left(\frac{2k}{Q}\right)^s\left[\prod_{n=0}^{(l-1)/2}\frac{s-(2n+1)}{s+2n}\right]\left[1+\frac{(l+s-1)(l-s+2)}{4(1-s)(k/Q)^2}+O(Q/k)^4\right]+\text{c.c.}\right\}, \tag{53}$$

which will play a crucial role in what follows to obtain the three-body parameter at nonzero R_*. In particular, Eq. (53) shows that $k^2D(\mathbf{k})$ is asymptotically an oscillating function of k/Q that is log-periodic: The same pattern is reproduced when k is multiplied by $\exp(2\pi/|s|)$. For $k^2D(\mathbf{k})$ to approach this asymptotic oscillating function, the very stringent condition $k/Q\gg\exp(2\pi/|s|)$ is, fortunately, not required; it is simply sufficient that $k/Q\gg 1$ (for l and $|s|$ not much larger than unity).

A second technique to calculate Eq. (50) is to use spherical coordinates of axis the quantization axis z. The integral over the azimuthal angle ϕ is straightforward. The integral over the modulus x can be performed if one uses the integral representation 8.432(1) of the Bessel function given in Ref. [31], $K_s(z)=\int_0^{+\infty}dt\,\exp(-z\cosh t)\cosh(st)$. In the integral over the polar angle θ, one replaces $Y_l^0(\mathbf{x})$ by its expression in terms of the Legendre polynomial $P_l(u)$ with the variable $u=\cos\theta$, and one integrates by parts the factor $1/(\cosh t+iku/Q)^2$ that appeared after integration over x. The integral over t can then be performed with contour integration:

$$\int_{-\infty}^{+\infty}\frac{dt}{2\pi}\frac{e^{-iSt}}{\cosh t+i\sinh\beta} = \frac{\sin[S(\beta+i\pi/2)]}{i\sinh(S\pi)\cosh\beta}, \tag{54}$$

where S and β are real quantities. Changing to the variable $\beta=\text{arsinh}(ku/Q)$ in the integral over u, one obtains

$$D(\mathbf{k}) = Y_l^0(\mathbf{k})\frac{2i\pi^2Q^2}{k\cosh(S\pi/2)}\left\{\frac{\cos[S\,\text{arsinh}(k/Q)]}{(k^2+Q^2)^{1/2}} -\frac{1}{k}\int_0^{\text{arsinh}(k/Q)}d\beta\,P_l'\left(\frac{Q\sinh\beta}{k}\right)\cos(S\beta)\right\}, \tag{55}$$

where we have set $s=iS$. Generalizing the technique of Sec. III A to the derivative P_l' of the Legendre polynomial allows a direct evaluation of $D(\mathbf{k})$ without the need of hypergeometric functions.

C. Case $R_*>0$ at zero energy

In this subsection, as in the previous one, we restrict our study to the case where an Efimov effect takes place: Based on the results of Sec. IV A, the angular-momentum quantum number l is odd and the mass ratio α is larger than the corresponding critical value $\alpha_c^{(l)}$, so the function $\Lambda_l(s)$ has a single purely imaginary root $s_l = iS_l$ with positive imaginary part,

$$\Lambda_l(iS_l) = 0 \quad \text{with} \quad S_l > 0. \tag{56}$$

As remarkably shown for three bosons in Ref. [12] the narrow Feshbach resonance model can be solved analytically at zero energy, which gives access to the three-body parameter, that is, to the energy scale in the asymptotically geometric Efimovian trimer spectrum.

The underlying idea of the solution is that, at zero energy and after division of the overall Eq. (32) by a factor k, the integral part of the resulting equation is strictly scale invariant. If one takes as variable the logarithm of k rather than k, this strict scale invariance corresponds to a translation invariance, which suggests that the integral part is simply a convolution product and leads one to perform a Fourier transform with respect to $\ln k$. More precisely, we use the following ansatz:

$$f^{(l)}(k) = e^{-2x}\, F^{(l)}(x) \quad \text{with} \quad x = \ln(kR_* \cos\nu), \tag{57}$$

where the factor e^{-2x} shall lead to a convolution kernel with the desired even function and $\cos\nu$ is a function of the mass ratio given by Eq. (38). Dividing Eq. (32) for $E = 0$ by k, injecting the ansatz of Eq. (57) into the resulting equation, and, finally, multiplying by e^{2x}, we obtain

$$0 = (1 + e^x)F^{(l)}(x)\cos\nu + \int_{-\infty}^{+\infty} dX\, \mathcal{K}_l(X - x)F^{(l)}(X) \tag{58}$$

with the kernel

$$\mathcal{K}_l(x) = \frac{1}{2\pi}\int_{-1}^{1} du \frac{P_l(u)}{\cosh(x) + \frac{\alpha}{1+\alpha}u}. \tag{59}$$

As expected, Eq. (58) is the convolution product. We thus introduce the Fourier representation of the function $F^{(l)}$ [36]:

$$F^{(l)}(x) = \int_{-\infty+i0^+}^{+\infty+i0^+} \frac{dS}{2\pi} e^{iSx}\, \tilde{F}^{(l)}(S). \tag{60}$$

We expect that the function $F^{(l)}(x)$ oscillates periodically for $x \to -\infty$: When $x \to -\infty$, the momentum k tends to 0, and it becomes much smaller than $1/R_*$. One enters a universal zero-energy, zero-range regime where solutions of the type (33) are obtained, with s purely imaginary for an Efimovian solution. According to Eq. (57), this implies that $F^{(l)}(x)$ has plane-wave oscillations at $x \to -\infty$, with a wave number $\pm S_l$ since both $s = iS_l$ and $s = -iS_l$ are roots of $\Lambda_l(s) = 0$. More precisely, we expect that there exist coefficients $A_\pm$ such that

$$F^{(l)}(x) \underset{x\to-\infty}{=} A_+ e^{iS_l x} + A_- e^{-iS_l x} + o(1). \tag{61}$$

This will be checked *a posteriori*. As a consequence, the Fourier transform $\tilde{F}^{(l)}(S)$ has singularities on the real axis. More precisely, Eq. (61) leads to the natural conclusion that

$$\tilde{F}^{(l)}(S) \text{ has simple poles in } S = \pm S_l. \tag{62}$$

This is why the integration contour in Eq. (60) is infinitesimally shifted upward in the complex plane. This is a standard procedure in physics; see, for example, the expression of the unitary evolution operator as a Fourier transform of the resolvent for a system with a time-independent Hamiltonian [37]. In this Fourier representation, the convolution becomes a product, and one needs to calculate the Fourier transform $\tilde{\mathcal{K}}_l(S)$ of the kernel function K. Exchanging the integration over u and x, one then recovers exactly the integral in Eq. (35) knowing that $s = iS$ in that equation so

$$\tilde{\mathcal{K}}_l(S) = \Lambda(iS) - \cos\nu. \tag{63}$$

The only subtle part is the determination of the Fourier representation of the function $x \to e^x F^{(l)}(x)$. Multiplying (60) by e^x gives

$$e^x F^{(l)}(x) = \int_{-\infty+i0^+}^{+\infty+i0^+} \frac{dS}{2\pi} e^{i(S-i)x}\, \tilde{F}^{(l)}(S). \tag{64}$$

This is not directly of the Fourier form of Eq. (60) because $S - i$ rather than S appears inside the exponential. Now, if the integrand, that is, here, in practice, the function $S \to \tilde{F}^{(l)}(S)$, is a meromorphic function with no singularities (no poles) in the band $0^+ \leqslant \operatorname{Im} z \leqslant 1 + 0^+$, that is, $0 < \operatorname{Im} z \leqslant 1$, where $z \in \mathbb{C}$, we can shift the integration contour in Eq. (64) upward by one unity along the vertical axis in the complex plane to replace $S - i$ with S. Under the hypothesis

$$\tilde{F}^{(l)}(z) \quad \text{has no singularities for} \quad 0 < \operatorname{Im} z \leqslant 1, \tag{65}$$

we thus have

$$e^x F^{(l)}(x) = \int_{-\infty+i0^+}^{+\infty+i0^+} \frac{dS}{2\pi} e^{iSx}\, \tilde{F}^{(l)}(S + i), \tag{66}$$

which is exactly of the Fourier functional form (60); that is, the function $S \to \tilde{F}^{(l)}(S + i)$ is the Fourier transform of the function $x \to e^x F^{(l)}(x)$. This procedure is summarized on Fig. 1, where the original [Eq. (64)] and shifted [Eq. (66)] integration contours are plotted and where the locations of the poles of $\tilde{F}^{(l)}(z)$ are also indicated. Equation (58) then reduces to

$$0 = \tilde{F}^{(l)}(S + i)\cos\nu + \Lambda_l(iS)\tilde{F}^{(l)}(S) \tag{67}$$

for all real S.

To solve Eq. (67) we follow Ref. [12]. We, first, introduce the ansatz

$$\tilde{F}^{(l)}(S) = \frac{\pi}{\sinh[\pi(S + S_l)]} C_l(S), \tag{68}$$

where we recall that iS_l is the positive-imaginary-part root of $\Lambda_l(s)$. The factor with the hyperbolic sine is carefully chosen to give a minus sinus under translation $S \to S + i$, *a priori* introducing poles in $z = -S_l$, $z = -S_l \pm i$, $z = -S_l \pm 2i$, etc., for the function $\tilde{F}^{(l)}(z)$. This does not introduce singularities in the band $0 < \operatorname{Im} z \leqslant 1$ provided that the function $C_l(z)$ tends to zero for $z \to -S_l + i$, a point to be checked *a posteriori*. The unknown function C_l solves

$$C_l(S + i)\cos\nu = \Lambda_l(iS)\, C_l(S) \tag{69}$$

on the real axis. According to the expectation of Eq. (62), the function $C_l(S)$ has no pole in $S = -S_l$, since the $1/\sinh$ factor in Eq. (68) already has a simple pole in $S = -S_l$, and $C_l(S)$ has a simple pole in $S = S_l$, since the $1/\sinh$ factor has no

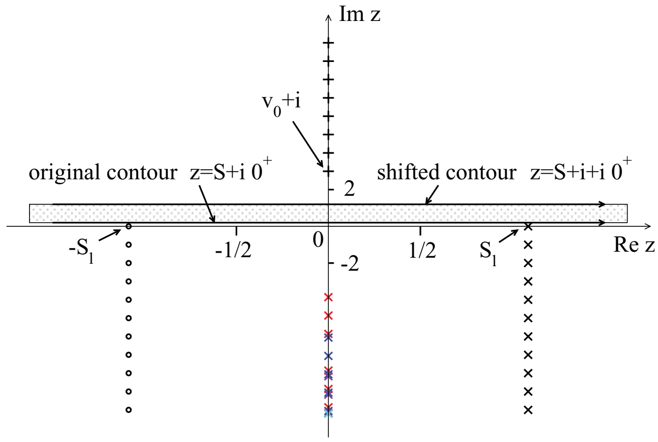

FIG. 1. (Color online) In the complex plane, illustration of the procedure used to determine the Fourier transform of the function $x \to e^x F^{(l)}(x)$: Under the *a posteriori* checkable hypothesis of Eq. (65) (no pole of $\tilde{F}^{(l)}(z)$ in the gray area), one can shift the integration contour in Eq. (64) upward by one unity along the vertical axis to obtain the Fourier representation [Eq. (66)] of $x \to e^x F^{(l)}(x)$. (Circles) Poles of $\tilde{F}^{(l)}(z)$ due to the function hyperbolic sine in the denominator of Eq. (68). (Pluses) Poles of $\tilde{F}^{(l)}(z)$ due to the factors $\Gamma(1+iz-iv_n)$, $n \geqslant 0$, in the numerators of the infinite product (71). (Black crosses) Poles of $\tilde{F}^{(l)}(z)$ due to the factor $\Gamma(iS_l - iz)$ in Eq. (71). Colored crosses on the $\mathrm{Im}\, z < 0$ part of the imaginary axis: Poles of $\tilde{F}^{(l)}(z)$ due to the factors $\Gamma(-iu_n - iz)$ for $n > 0$ in Eq. (71) [(red) $n = 1$; (blue) $n = 2$; (violet) $n = 3$; (cyan) $n = 4$]; from top to bottom, $n = 1$ (three crosses), $n = 2$ (two crosses), two triplets $n = 1,2,3$, and a quadruplet $n = 1,2,3,4$. The figure corresponds to $l = 1$ and $\alpha = 20$.

pole there [38]. As in Ref. [12] one then uses the Weierstrass representation

$$\Lambda_l(iS) = \cos\nu \prod_{n\in\mathbb{N}} \frac{S^2 - u_n^2}{S^2 - v_n^2}, \tag{70}$$

where the overall factor $\cos\nu$ is the limit of $\Lambda_l(iS)$ for $S \to \infty$; see Eq. (42). In Eq. (70), $u_0 = S_l$ is the real positive root of the function $S \to \Lambda_l(iS)$, $-u_0$ is the real negative root, and the $\pm u_n$, $n \geqslant 1$, are the purely imaginary roots of $S \to \Lambda_l(iS)$, $\mathrm{Im}\, u_n > 0$. The u_n's are sorted by ascending order of their imaginary parts, and, for general values of the mass ratio α, they form an irregular, aperiodic sequence. They, of course, depend on the angular momentum l. On the contrary, for general values of the mass ratio α, the poles of $S \to \Lambda(iS)$ are found from Eq. (41) to simply be $\pm v_n$, with $v_n = i(2n + l + 1)$ for all integers $n \geqslant 0$ [39]. Finally, one can check as in Ref. [12] that the function C_l is given by the infinite product

$$C_l(S) = \frac{\Gamma(iS_l - iS)\Gamma(1+iS-iv_0)}{\Gamma(1+iS+iS_l)\Gamma(-iS-iv_0)} \times \prod_{n\in\mathbb{N}^*} \frac{\Gamma(-iS-iu_n)\Gamma(1+iS-iv_n)}{\Gamma(-iS-iv_n)\Gamma(1+iS-iu_n)}, \tag{71}$$

where we recall that the u_n and v_n depend on l. In particular, one can check that this expression vanishes for $S \to -S_l + i$, as required above Eq. (69), and has no pole in the band $0 < \mathrm{Im}\, z \leqslant 1$ of the complex plane [40]. Together with Eq. (68), this constitutes the desired solution at zero energy for $R_* > 0$.

An important application of this result is to calculate the previously mentioned low-k or $x \to -\infty$ behavior [Eq. (61)] of the solution [41], which is a universal regime that has to match the zero-range model. Since $x < 0$, in applying the usual contour integration technique to Eq. (60), we close the integration contour following a half-circle in the lower part $\mathrm{Im}\, z < 0$ of the complex plane. According to the Cauchy residue formula, one gets for $F^{(l)}(x)$ a sum of terms proportional to $e^{iz_n x}$, where the sum is taken over all poles z_n of the integrand in the lower half-plane (see the pole locations in Fig. 1). For $x \to -\infty$, the poles with a nonzero imaginary part have a contribution that vanishes as $O(e^x)$, and the sum is dominated by the two poles $z = \pm S_l$ on the real axis, which are the only ones to give purely oscillating, nondecaying contributions. The corresponding residues of $\tilde{F}^{(l)}(S)$ can be deduced from

$$\tilde{F}^{(l)}(S) \underset{S\to -S_l}{\sim} \frac{C_l(-S_l)}{S+S_l} \quad \text{and} \quad \tilde{F}^{(l)}(S) \underset{S\to S_l}{\sim} \frac{[C_l(-S_l)]^*}{S-S_l}. \tag{72}$$

The value of the first residue directly results from the ansatz of Eq. (68) and the absence of pole of the function $C_l(S)$ in $S = -S_l$. If one further uses Eq. (69) for $S \to S_l$, one finds for the second residue $[\pi/\sinh(2\pi S_l)]C_l(S_l + i)\cos\nu/i\Lambda_l'(iS_l)$. Properties of the explicit form of Eq. (71) and of the Γ function, as in Ref. [12], lead to Eq. (72) [42]. Finally, turning back to the k variable and to the function D:

$$D(\mathbf{k}) \underset{kR_*\to 0^+}{=} -i\left(\frac{Q}{qR_*k}\right)^2 Y_l^0(\mathbf{k})\left\{[C_l(-S_l)]^*(qR_*k/Q)^{iS_l} + \text{c.c.} + O(qR_*k/Q)\right\}, \tag{73}$$

where we recall that $S_l > 0$ and $q/Q = \cos\nu$ as in Eq. (47). The asymptotic form in the right-hand side of Eq. (73) is satisfactory: It is indeed a superposition of solutions of the zero-range model at zero energy; see Eq. (33). A first important point is that it is actually a *specific* linear combination of the solutions with exponents $s = \pm iS_l$, with relative amplitudes depending on the Feshbach length R_*. This selection of the right linear combination amounts to adjusting the three-body parameter to its right value in the Danilov three-body contact conditions [28]. Equation (73) thus constitutes a microscopic derivation of this three-body parameter in the limit of an infinitely narrow Feshbach resonance [11,12]. A second important point is that the solution $D(\mathbf{k})$ starts approaching the log-periodic oscillatory asymptotic form $(kR_*\cos\nu)^{\pm iS_l}$ as soon as $kR_*\cos\nu < 1$, and there is no need to require that $kR_*\cos\nu < e^{-2\pi/S_l}$. There is no need to require that the oscillatory form has performed at least one oscillation to have $D(\mathbf{k})$ well approximated by it.

IV. ANALYTICAL RESULTS ON TRIMER STATES

In this section, we develop a physical application of the particular analytical solutions of the previous section. From the zero-energy and zero-range solution, we first determine, for each value of the angular momentum l, the critical mass ratio $\alpha_c^{(l)}$ leading to the Efimov effect and the corresponding purely imaginary Efimov exponent $s_l = iS_l$, with the convention $S_l > 0$. Accurate asymptotic estimates for these quantities are obtained and are compared to the Born-Oppenheimer approximation. Second, from a matching of the ($E < 0, R_* = 0$) solution to the ($E = 0, R_* > 0$) solution, we determine the Efimovian part of the spectrum, in particular, the global energy scale $E_{\rm global}^{(l)}$ appearing in that geometric spectrum. The dependence of $E_{\rm global}^{(l)}$ on the mass ratio, close to the Efimov threshold $\alpha \to \alpha_c^{(l)}$ and arbitrarily far from it ($\alpha \to +\infty$), is studied. Also the variation of $E_{\rm global}^{(l)}$ with the angular momentum l, in particular for α close to the critical mass ratio $\alpha_c^{(l)}$, is analyzed. Third, using the Born-Oppenheimer approximation expected to be asymptotically exact for a diverging mass ratio, we show that the hydrogenoid character gradually takes over the Efimovian character in that limit, except in a vicinity of the $E = 0$ accumulation point (which remains Efimovian).

A. Efimovian threshold $\alpha_c^{(l)}$ and exponent s_l

As a physical application of Eqs. (41), (42), and (44), we determine the values of the mass ratio α and of the angular momentum l such that the Efimov effect takes place; that is, the transcendental equation $\Lambda_l(s) = 0$ admits some purely imaginary solutions.

A useful guide is the Born-Oppenheimer approximation [5] that becomes exact in the limiting cases of vanishing or diverging mass ratio α. It indicates that the Efimov effect should take place for large-enough values of α and for odd values of l. In the limit $\alpha \to 0$, the extra particle is, indeed, infinitely massive, so the fermions see a fixed pointlike scatterer with infinite scattering length, which does not support bound states. In the opposite limit $\alpha \to +\infty$, the extra particle sees the very massive fermions as two fixed pointlike scatterers of positions $\mathbf{r}_2$ and $\mathbf{r}_3$, with which it forms a single bound state, of energy

$$\epsilon_0(r_{23}) = -\frac{\hbar^2 C^2}{2 M r_{23}^2} \tag{74}$$

in the zero-range Bethe-Peierls model, and with a wave function that is symmetric under the exchange of $\mathbf{r}_2$ and $\mathbf{r}_3$. Here the constant C obeys

$$C = \exp(-C) \quad \text{so} \quad C = 0.567\,143\,290\,409\ldots. \tag{75}$$

It can be related to the Lambert function by $C = W(1)$, and it is sometimes called the Ω constant. Since the global state vector is fermionic, this extra-particle wave function can be combined in the Born-Oppenheimer factorized form with an odd orbital fermionic part only. The effective potential seen by the fermions is, thus, the sum of the Born-Oppenheimer potential $\epsilon_0(r_{23})$ and of the angular-momentum centrifugal part $\hbar^2 l(l+1)/(m r_{23}^2)$. In three dimensions, the zero-energy solution in that effective potential has to be written as $r_{23}^{s-1/2}$ to match the usual definition of the Efimov exponent which is given in two dimensions [43]. We then obtain the Born-Oppenheimer approximation for the root s,

$$s_{\rm BO}^2 = \left(l + \tfrac{1}{2}\right)^2 - \tfrac{1}{2}\alpha C^2 \quad (l \text{ odd}), \tag{76}$$

to be used in the regime where $s_{\rm BO}^2 \leqslant 0$. Interestingly, this Born-Oppenheimer approximation can also be used for a nonzero R_* to obtain exact results on the non-Efimovian low-energy trimers for $\alpha \to +\infty$, as developed in Sec. IV C.

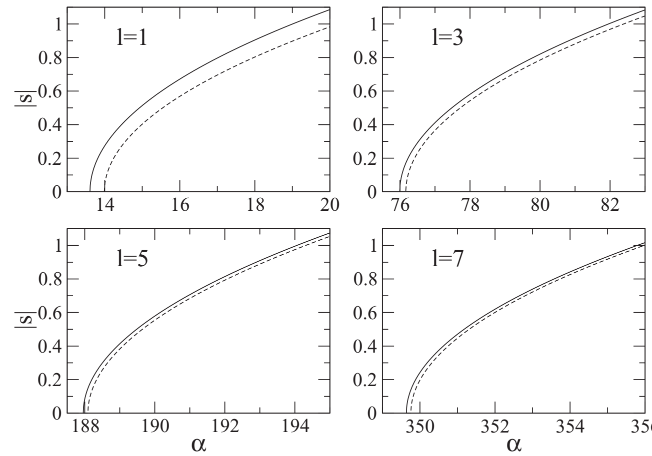

FIG. 2. Values of the Efimov exponent s as a function of the fermion-to-extra-particle mass ratio $\alpha = m/M$ for several values of the angular momentum l. The modulus of s is shown only over the interval of mass ratio where s is purely imaginary (that is, where the Efimov effect takes place). This was found to occur only for odd values of l, and for a single pair of $\pm s$ roots of $\Lambda_l(s) = 0$. (Solid line) Numerical result from the exact function $\Lambda_l(s)$ as given by Eq. (42). (Dashed line) Born-Oppenheimer approximation [Eq. (76)].

Turning back to the exact equation $\Lambda_l(s) = 0$: For a fixed value of l, we expect that the solutions s of the transcendental equation are continuous functions of the mass ratio α. The critical values $\alpha_c^{(l)}$ of α for the emergence of the Efimov effect are, thus, such that $\Lambda_l(0) = 0$. From a numerical calculation of $\Lambda_l(s = 0)$ as a function of α ranging from 0 to $+\infty$, we indeed find, for even l, that $\Lambda_l(s = 0)$ has a constant positive sign, which means the absence of the Efimov effect. For each odd l, we find that $\Lambda_l(s = 0)$ changes sign once (from positive to negative for increasing α). The resulting values of $\alpha_c^{(l)}$ are, for example,

$$\begin{aligned} \alpha_c^{(l=1)} &= 13.60696\ldots, \quad \alpha_c^{(l=3)} = 75.99449\ldots \\ \alpha_c^{(l=5)} &= 187.9583\ldots, \quad \alpha_c^{(l=7)} = 349.6384\ldots. \end{aligned} \tag{77}$$

The critical mass ratio for $l = 1$ is given in Ref. [5] and in Ref. [44] for $l = 3$ and $l = 5$. For larger l we have checked that $[\alpha_c^{(l)} C^2/2]^{1/2}$ is indeed very close to the approximation $l + 1/2$ resulting from Eq. (76). For these few odd values of l, we then solve numerically $\Lambda_l(iS) = 0$, where $S > 0$, to obtain the Efimov exponent as a function of α for $\alpha > \alpha_c^{(l)}$. For each values of l and $\alpha > \alpha_c^{(l)}$, it is observed that $\Lambda_l(iS)$ for $S > 0$ is an increasing function of S, so a single pair of $\pm i S_l$ imaginary roots is obtained. The results are shown as solid lines in Fig. 2. For comparison, the Born-Oppenheimer approximation of Eq. (76) is plotted as dashed lines in that figure. As expected intuitively, it approaches the exact result in the large l (and, thus, large α) limit.

One can, however, be more precise in the evaluation of the accuracy of Eq. (76). For a *fixed* value $s_l = i S_l$ of the Efimov exponent, one can perform a large l expansion of the mass ratio, as shown in Appendix D, to obtain

$$\tfrac{1}{2} C^2 \left(\alpha - \alpha_c^{(l)}\right) \underset{l \to \infty}{=} S_l^2 [1 + O(1/l)], \tag{78}$$

where the critical mass ratio $\alpha_c^{(l)}$ has the large l expansion

$$\tfrac{1}{2}C^2\alpha_c^{(l)} \underset{l\to\infty}{=} \left(l+\tfrac{1}{2}\right)^2 + \Delta + O(1/l). \tag{79}$$

Δ is, thus, the first correction to the critical mass ratio predicted by the Born-Oppenheimer approximation of Eq. (76). Accidentally, it has a very small numerical value [45]:

$$\Delta = \frac{17-C^2}{12} - \frac{7}{6}\left(C + \frac{1}{C+1}\right) = -0.016\,259\,165\ldots \tag{80}$$

so the Born-Oppenheimer approximation for $\alpha_c^{(l)}$ is, in practice, quite good for large l. For $\alpha \to +\infty$ for a *fixed* angular momentum l, one can also obtain from the results of Appendix E the following asymptotic expansion for the imaginary root iS_l of $\Lambda_l(s)$:

$$S_l^2 \underset{\alpha\to+\infty}{=} \frac{C^2}{2}\alpha - \left(l+\frac{1}{2}\right)^2 + \delta + O(1/\alpha), \tag{81}$$

where the first two terms in the right-hand side constitute the Born-Oppenheimer approximation and the angular-momentum-independent constant δ differs from zero,

$$\delta = \frac{5}{12}C^2 + \frac{4}{3}\frac{C^2}{1+C} + \frac{1}{4} = 0.657\,684\ldots. \tag{82}$$

Note that Eq. (81) is not in contradiction with Eq. (78) [combined with Eq. (79)] because the considered limits differ totally; S_l/l either diverges or vanishes. As s^2 is a coefficient in the Born-Oppenheimer potential, a suggestive picture obtained from Eq. (81) is that the Born-Oppenheimer approximation has an error $O(\alpha^0)$ on the effective potential seen by the fermions. Mathematically, Eq. (81) shows that the error on S_l due to the Born-Oppenheimer approximation vanishes as $1/\alpha^{1/2}$ and that the approximation gets the correct leading term $\alpha^{1/2}$ and the correct subleading term α^0 (which turns out to vanish) in an asymptotic expansion of S_l in powers of $\alpha^{1/2}$. These remarks are useful for Sec. IV C.

B. Efimovian part of the trimer spectrum

In presence of the Efimov effect, we have obtained so far two solutions to the integral Eq. (32) in limiting cases; see Sec. III B for $R_* = 0, E < 0$, and Sec. III C for $R_* > 0, E = 0$. How can we then obtain an approximation for the corresponding spectrum of trimers, which requires both $R_* > 0$ and $E < 0$?

Roughly speaking, and dropping, for simplicity, a possible dependence on the mass ratio α of the various bounds, the solution of Sec. III B is expected to constitute an accurate approximation of the trimer solution at interparticle distances much larger than R_*, that is, at momenta smaller than $\hbar/R_*$. In a symmetric manner, the solution of Sec. III C is expected to well approximate the trimer solution at short-enough interparticle distances, smaller than $1/q$, where the $E < 0$ wave function only weakly departs from the zero-energy one. This corresponds to momenta much larger than $\hbar q$. There thus exists an interval of momentum $\hbar k$ over which both limiting solutions are close to the physical trimer solution, $q \ll k \ll 1/R_*$, if

$$qR_* \ll 1. \tag{83}$$

In this case, we can match the two limiting solutions, as summarized in Fig. 3. Over this matching interval of momentum, one has $k \gg q$ so the solution of Sec. III B is in its large k regime given by Eq. (53) with $s = iS_l$. Over this interval, one also has $k \ll 1/R_*$, so the solution of Sec. III C is in its low-k regime given by Eq. (73). These two limiting regimes are compatible (within an arbitrary normalization factor) if q is of the form [46]

$$q_n^{(l)} = q_{\text{global}}^{(l)} e^{-\pi n/|s_l|}, \quad n \text{ integer}, \tag{84}$$

where we recall that the Efimov exponent is $s_l = iS_l$, $S_l > 0$ and the trimer energy is $E = -\hbar^2q^2/(2\mu)$, with $\mu = mM/(m+M)$. Equation (84) is the expected geometric Efimovian spectrum, and we have the explicit expressions for the corresponding global wave number and energy scales:

$$q_{\text{global}}^{(l)} = \frac{2}{R_*}e^{\theta_l/|s_l|} \quad\text{and}\quad E_{\text{global}}^{(l)} = -\frac{2\hbar^2}{\mu R_*^2}e^{2\theta_l/|s_l|}, \tag{85}$$

where θ_l is the phase of the complex number

$$Z_l = |Z_l|e^{i\theta_l} \equiv \left[\prod_{n=1}^{l}(n-s_l)\right]s_l C_l(-S_l) \tag{86}$$

and the function $C_l(S)$ is given by Eq. (71). At fixed angular momentum, the phase θ_l depends on the mass ratio $\alpha = m/M$. For α tending from above to the critical value $\alpha_c^{(l)}$, $S_l \to 0$, we show in Appendix B that Z_l tends to a real and positive number. We thus choose the usual determination $\theta_l = \arg Z_l$ in that limit and extend it by continuity to all larger values of α.

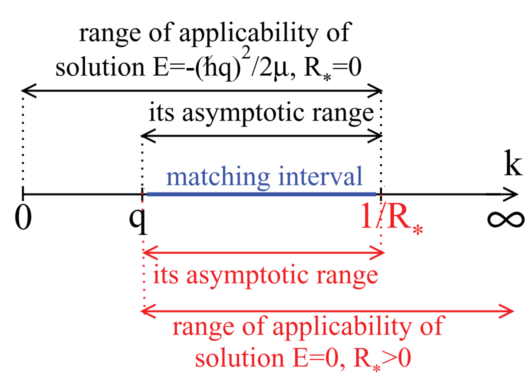

FIG. 3. (Color online) Matching of two limiting solutions of the integral Eq. (32), the solution $E = -\hbar^2q^2/(2\mu) < 0, R_* = 0$ (see text in black, in the upper half of the figure) given by Eq. (52) and the solution $E = 0, R_* > 0$ (see the text in red in the lower half of the figure) deducible from Eqs. (27), (57), (60), (68), and (71), over a common interval of values of k (the "matching interval," blue segment on k axis) where they are both in their asymptotic regimes, Eqs. (53) and (73). This matching procedure leads to the Efimovian spectrum formula (84) with a global scale given by Eq. (85). This procedure makes sense when $qR_* \ll 1$, and it is expected to be exact when $qR_* \to 0$, that is, for the quantum number n tending to infinity for a fixed (purely imaginary) Efimov exponent s_l (as in Efimov's historical solution) or (less usually) for $|s_l|$ tending to zero at fixed quantum number $n \geqslant 1$. For simplicity of the figure, we have dropped factors slowly depending on the mass ratio α, such as $\cos\nu$; that is, we have assumed that the angular momentum l and $|s_l|$ are not much larger than unity.

For the analytical developments that follow, obtained for the global scale $q_{\rm global}^{(l)}$ in the limit of large angular momenta for $\alpha-\alpha_c^{(l)}$ fixed, or in the limit of a large mass ratio at fixed angular momentum, there is a more operational expression for θ_l that does not require the determination of all the roots and poles of $\Lambda_l(iS)$ to evaluate $C_l(-S_l)$. As shown in Appendix C, one has the series representation of the phase θ_l of Z_l:

$$\theta_l = \mathrm{Im}[\ln\Gamma(1+iS_l)+\ln\Gamma(1+2iS_l)+2\ln\Gamma(l+1-iS_l)+\ln\Gamma(l+2-iS_l)] + \int_0^{S_l} dS \ln\left[\frac{\Lambda_l(iS)}{\cos\nu}\frac{S^2+(l+1)^2}{S^2-S_l^2}\right] + \sum_{k\geqslant 1}\frac{(-1)^k B_{2k}}{(2k)!}\frac{d^{2k-1}}{dS^{2k-1}}\left\{\ln\left[\frac{\Lambda_l(iS)}{\cos\nu}\frac{S^2+(l+1)^2}{S^2-S_l^2}\right]\right\}_{S=S_l}, \tag{87}$$

where we recall that S_l is the positive root of the function $\Lambda_l(iS)$ and the B_k are Bernoulli's numbers, $B_1=-1/2, B_2=1/6,\ldots$. Since Eq. (87) was obtained from Stirling's series, which is an *asymptotic* series, we expect that Eq. (87) is also an asymptotic series. We thus investigated numerically how many terms one has to keep in practice to have good accuracy. Figure 4(a) shows that the zeroth-order approximation, consisting in omitting *all* the terms in the sum over k in Eq. (87), already gives, in practice, a sufficiently accurate approximation for the global scale $q_{\rm global}^{(l)}$. In Fig. 4(b), it is shown that the difference between the exact value of θ_l, obtained from the infinite product representation of $C_l(-S_l)$, and the zeroth-order approximation, omitting all k terms in Eq. (87), is nonzero but is very accurately accounted for by the term $k=1$ in Eq. (87).

From the zero-range theory by Efimov, it is expected that the geometric form Eq. (84) of the spectrum is asymptotically exact in the limit of a large quantum number, $n\to+\infty$; see the constraint [Eq. (83)]. How large the values of n should be to reach this geometric behavior will be evaluated numerically in Sec. V [in the mean time, see the discussion that follows Eq. (89)]. The advantage of the nonzero R_* calculation is that it also gives the global energy scale in the spectrum; see the factor $q_{\rm global}^{(l)}$ in Eq. (84) explicitly given by Eq. (85). As compared to the bosonic case [11,12], there is an additional knob here, which is the mass ratio α. How does the global energy scale vary with the mass ratio?

For $\alpha\to\alpha_c^{(l)}$: The behavior of the global energy scale close to the critical mass ratio can be determined from the results of Appendix B, where it is shown that θ_l vanishes linearly with S_l:

$$\lim_{\alpha\to\alpha_c^{(l)}}\frac{\theta_l}{|s_l|} = -\psi(l+1)+3\psi(1)-\psi(-iv_0)-\psi(1-iv_0) + \sum_{n=1}^{+\infty}\left[\psi\left(-iu_n^c\right)+\psi\left(1-iu_n^c\right)-\psi\left(-iv_n\right)-\psi\left(1-iv_n\right)\right], \tag{88}$$

where $u_n^c, n>0$ is the value of the complex root u_n of the function $S\to\Lambda_l(iS)$ at the critical mass ratio; the $v_n=i(2n+l+1)$, $n\geqslant 0$, are the poles of $S\to\Lambda_l(iS)$; and the function $\psi(z)$ is the digamma function, that is, the logarithmic derivative of the Γ function. As a consequence, the global energy scale has a finite limit at the threshold for the Efimov effect! We give here a few corresponding values obtained from the rapidly converging formula (B6):

$$q_{\rm global}^{(l=1)}R_*\simeq 6.56577\times10^{-2},\quad q_{\rm global}^{(l=3)}R_*\simeq 6.12349\times10^{-3}$$
$$q_{\rm global}^{(l=5)}R_*\simeq 1.62809\times10^{-3},\quad q_{\rm global}^{(l=7)}R_*\simeq 6.48952\times10^{-4}. \tag{89}$$

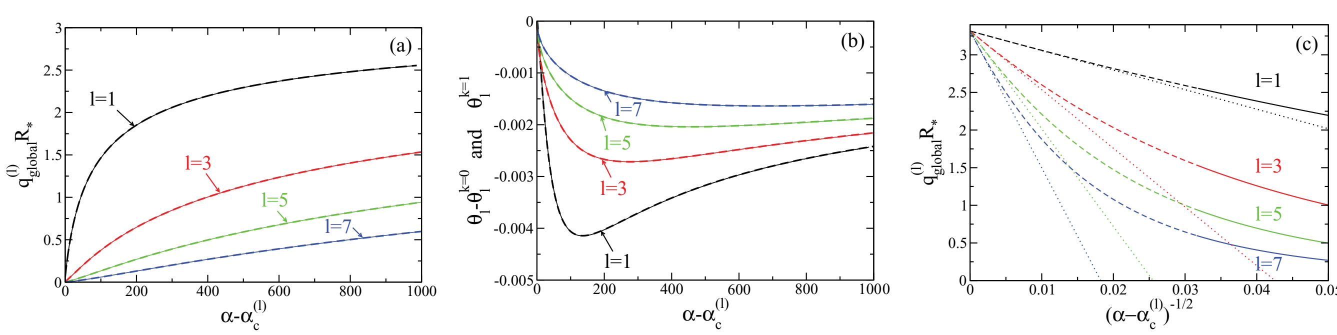

FIG. 4. (Color online) In (a) value of the global wave-number scale $q_{\rm global}^{(l)}$ of the Efimovian part of the spectrum [see Eq. (85)] as a function of the difference of the mass ratio α from its critical value, for all odd angular momenta up to $l=7$. (Thin solid lines) Exact result obtained from Eq. (86) and from the infinite product representation Eq. (71) [the more rapidly converging form, Eqs. (C3) and (C5), was used in the numerics]. (Thick dashed lines) Zeroth-order approximation omitting all the terms in the sum over k in Eq. (87). In (b) the (small) difference between the exact θ_l and the zeroth-order approximation $\theta_l^{k=0}$ is plotted as thin solid lines, and the value $\theta_l^{k=1}$ of the $k=1$ term of Eq. (87) is plotted as thick dashed lines. In (c) the values of $q_{\rm global}^{(l)}$ resulting from the Born-Oppenheimer-plus-semiclassical approximation are shown as dashed lines [see Eq. (106)], as functions of $1/(\alpha-\alpha_c^{(l)})^{1/2}$, showing how the l-independent $\alpha\to+\infty$ limit is reached. The solid lines correspond to the exact numerical data of (a) and the dotted straight lines correspond to the asymptotic expansion [Eq. (108)].

At this threshold, $|s_l| \to 0$ so we expect that Eq. (84) actually becomes exact for the quantum number $n \geqslant 1$, since $q_n^{(l)} R_*$ tends to zero in that limit, whereas Eq. (84) is clearly invalid for $n \leqslant -1$. The case $n = 0$ is dubious: Although $q_0^{(l)} R_*$ does not tend to zero at the threshold, it assumes very small values, so maybe Eq. (84) still makes sense. We cannot, however, say more at this stage, and the question of whether the quantum number $n = 1$ corresponds to the ground trimer state (for a given angular momentum l) will be answered in Sec. V.

For $l \to +\infty$: Another interesting question is to determine how $q_{\text{global}}^{(l)}$ depends on the angular momentum l at a fixed distance of the mass ratio α from the critical value $\alpha_c^{(l)}$, that is, roughly at constant values of the Efimov exponent s_l. After a numerical evaluation of Eq. (85), as detailed in Ref. [39], we found that $q_{\text{global}}^{(l)}$ drops rapidly for increasing l, roughly as $1/(\alpha_c^{(l)})^{3/2}$. According to Eq. (76) the critical mass ratio scales approximately as $(l + 1/2)^2$, so we expect that $q_{\text{global}}^{(l)}$ approximately scales as $1/(l + 1/2)^3$, an approximation that becomes rapidly excellent with increasing l as soon as l exceeds unity; see Fig. 5.

The scaling of $q_{\text{global}}^{(l)}$ as $1/l^3$ at a fixed distance from the critical mass ratio can be obtained analytically for $l \to +\infty$ using Eq. (87) for the angle θ_l and Eq. (44) for $\Lambda_l(iS)$, as detailed in Appendix D:

$$q_{\text{global}}^{(l)} R_* \underset{l\to+\infty}{\overset{\alpha-\alpha_c^{(l)}\ \text{fixed}}{\sim}} \frac{(1+C)\, e^{3\gamma}}{l^3} \exp\left\{ \frac{\text{Im}\,[\ln\Gamma(1+iS_l) + \ln\Gamma(1+2iS_l)]}{S_l} \right\}, \tag{90}$$

where $\gamma = 0.577\,215\,664\,9\ldots$ is Euler's constant and $s_l = iS_l$, $S_l > 0$. In that limit, one can use the Born-Oppenheimer-type relation, $S_l^2 = (\alpha - \alpha_c^{(l)})C^2/2$, as shown by Eq. (78). The asymptotic result [Eq. (90)] is plotted as a dashed line in Fig. 5 and well reproduces the large-l numerical results.

For $\alpha \to +\infty$: The behavior of the global energy scale in the limit of an infinite mass ratio (for a given l) is determined in Appendix E. It is found that $q_{\text{global}}^{(l)}$ has a finite limit, which remarkably is also independent of the angular momentum l:

$$q_{\text{global}}^{(l)} R_* \underset{\alpha\to+\infty}{\to} 2(1+C)\, e^J = 3.31582\ldots, \tag{91}$$

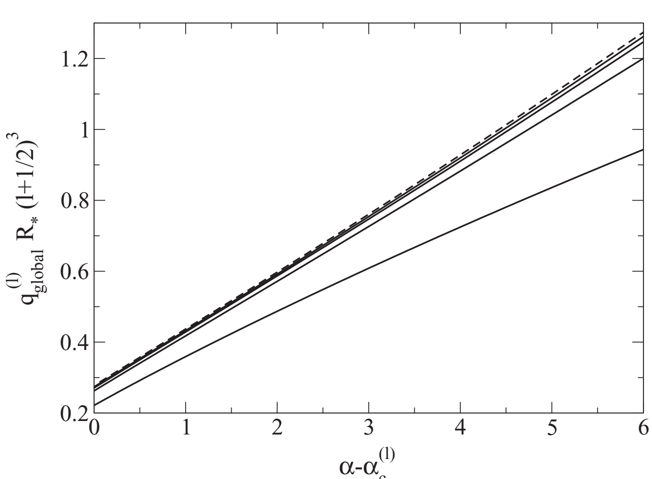

FIG. 5. Dependence, with the angular momentum l, of the global wave-number scale $q_{\text{global}}^{(l)}$ in the Efimov trimer spectrum, as obtained from the exact result (85). The figure shows the quantity $q_{\text{global}}^{(l)} R_*$ multiplied by $(l + 1/2)^3$, as a function of $\alpha - \alpha_c^{(l)}$, for (odd) angular momenta equal to $l = 1$, $l = 3$, $l = 5$, and $l = 7$, from bottom to top. This quantity is observed to converge rapidly to a finite limit for increasing l. The dashed line represents the analytical prediction (90) for that limit. We recall that $E_{\text{global}} = -\hbar^2 q_{\text{global}}^2/(2\mu)$.

where C is defined by Eq. (75) and J is the integral

$$J = \int_0^C dx \left[\frac{1}{C} \frac{1+x}{1-xe^x} - \frac{1}{C-x} \right] = 0.05630577\ldots. \tag{92}$$

As we shall see in Sec. IV C, for $\alpha \to +\infty$, the low-lying part of the trimer spectrum is hydrogenoid rather than Efimovian, so Eq. (91) is relevant only for trimers with diverging quantum number n.

C. Born-Oppenheimer approximation and hydrogenoid trimer spectrum

As explained in Sec. IV A the Born-Oppenheimer approach is a natural tool when the fermions become arbitrarily massive. The extra particle then mediates an attractive interaction potential $\epsilon(r_{23})$ between the heavy fermions, with $\mathbf{r}_{23} = \mathbf{r}_2 - \mathbf{r}_3$ the relative coordinates of the fermions. We calculate this interaction potential on a narrow Feshbach resonance. From Schrödinger's equation for the relative wave function of the two fermions,

$$E\psi(\mathbf{r}_{23}) = -\frac{\hbar^2}{m}\Delta_{\mathbf{r}_{23}}\psi(\mathbf{r}_{23}) + \epsilon(r_{23})\psi(\mathbf{r}_{23}), \tag{93}$$

which is in the odd l sector due to fermionic antisymmetry, we then determine the low-energy trimer states in the limit $\alpha \to +\infty$.

We first fix the positions of the fermions to $\mathbf{r}_2$ and $\mathbf{r}_3$. Each fermion then acts on the extra particle as a fixed scatterer of infinite scattering length, zero true range but finite effective range $r_e = -2R_*$. The effect of such a scatterer is then represented by modified contact conditions on the wave function $\phi(\mathbf{r}_1)$ of the extra particle in the so-called effective range approach [7,47]. For a bound state $\phi(\mathbf{r}_1)$ of eigenenergy

$$\epsilon(r_{23}) = -\frac{\hbar^2\kappa^2}{2M}, \tag{94}$$

where the dependence of $\kappa > 0$ on r_{23} is, for simplicity, omitted in the writing, we impose the boundary conditions

$$\phi(\mathbf{r}_1) \underset{\mathbf{r}_1\to\mathbf{r}_n}{=} A_n\left[\frac{1}{|\mathbf{r}_1-\mathbf{r}_n|}-\frac{1}{a_{\rm eff}}\right]+O(|\mathbf{r}_1-\mathbf{r}_n|) \quad (95)$$

in the vicinity of each scatterer $n = 2,3$. The effective scattering length is energy dependent, as $1/a_{\rm eff} = 1/a - k^2 r_e/2$ for an incoming free wave of wave number k. Here the true scattering length a is infinite, the effective range is $r_e = -2R_*$ for a narrow Feshbach resonance, and $k = i\kappa$ is purely imaginary for a bound state, so $1/a_{\rm eff} = -\kappa^2 R_*$. In the presence of the contact conditions, the extra-particle wave function obeys Schrödinger's equation

$$\epsilon(r_{23})\phi(\mathbf{r}_1) = -\frac{\hbar^2}{2M}\left[\Delta_{\mathbf{r}_1}\phi(\mathbf{r}_1)+\sum_{n=2}^{3}4\pi A_n\delta(\mathbf{r}_1-\mathbf{r}_n)\right], \quad (96)$$

where the Dirac terms are due to the $1/|\mathbf{r}_1 - \mathbf{r}_n|$ divergences. The general solution is expressed in terms of the Green's function of the Laplacian at negative energy:

$$\phi(\mathbf{r}_1) = \sum_{n=2}^{3} A_n\frac{e^{-\kappa|\mathbf{r}_1-\mathbf{r}_n|}}{|\mathbf{r}_1-\mathbf{r}_n|}. \quad (97)$$

The contact conditions [Eq. (95)] then impose $(1 + \kappa R_*)A_{2,3} = A_{3,2}e^{-\kappa r_{23}}/(\kappa r_{23})$. This 2×2 system has a nonzero solution only for the *symmetric* case $A_2 = A_3$, where κ solves

$$1+\kappa R_* = \frac{e^{-\kappa r_{23}}}{\kappa r_{23}}. \quad (98)$$

The wave function $\phi(\mathbf{r}_1)$ is then symmetric under the exchange of $\mathbf{r}_2$ and $\mathbf{r}_3$. As the Born-Oppenheimer ansatz for the total wave function is $\psi(\mathbf{r}_{23})\phi(\mathbf{r}_1;\mathbf{r}_2,\mathbf{r}_3)$, where the parametric dependence of ϕ with the fermions positions is made explicit, fermionic exchange symmetry indeed imposes $\psi(-\mathbf{r}_{23}) = -\psi(\mathbf{r}_{23})$.

For a fixed r_{23}, Eq. (98) looks difficult to solve. However, one can see that, for each positive κ, it is solved by a single positive r_{23} [48]. Furthermore, rewriting κ in the left-hand side as $(\kappa r_{23})/r_{23}$, r_{23}/R_* may be expressed as an explicit function of $u = \kappa r_{23}$, where u ranges from 0 to the numerical constant C defined in (75):

$$\frac{r_{23}}{R_*} = \frac{u^2}{e^{-u}-u}. \quad (99)$$

This allows a straightforward plot and study of the Born-Oppenheimer potential $\epsilon(r_{23})$. We reach, in particular, the useful limiting cases

$$\epsilon(r_{23}) \underset{r_{23}\to+\infty}{\sim} -\frac{\hbar^2C^2}{2Mr_{23}^2}, \quad (100)$$

$$\epsilon(r_{23}) \underset{r_{23}\to 0}{=} -\frac{\hbar^2}{2MR_*^2}\left[\frac{R_*}{r_{23}}-\frac{2R_*^{1/2}}{r_{23}^{1/2}}+O(1)\right]. \quad (101)$$

The asymptotic behavior of Eq. (100) reproduces the Born-Oppenheimer potential [Eq. (74)] obtained for the usual Bethe-Peierls case $R_* = 0$. For a large-enough α, and for each odd values of the angular momentum l, it ensures that the spectrum of Eq. (93) is indeed Efimovian in the limit of large quantum number n, that is, for $E \to 0^-$. On the contrary, for fixed quantum numbers n and l, the bound states of Eq. (93) for increasing $\alpha = m/M$ are increasingly localized in the low r_{23} part Eq. (101) of the Born-Oppenheimer potential. This means that the low-energy part of the spectrum is hydrogenoid; it becomes asymptotically equivalent for large α to the known spectrum of the hydrogen atom if one takes for the electron mass $m_e = m/2$ and the CGS electron charge e such that $e^2 = \hbar^2/(2MR_*)$. In terms of the wave number q introduced in Eq. (24), we thus obtain the exact asymptotic result [49]

$$q_n^{(l)}R_* \underset{\alpha\to+\infty}{\sim} \left(\frac{\alpha}{8}\right)^{1/2}\frac{1}{n+l}, \quad (102)$$

where the integer quantum number n start from $n = 1$ in each odd angular momentum sector l, so the hydrogen spectrum reads $-m_e e^4/[2\hbar^2(n+l)^2]$ with this convention.

Since the eigenfunctions of the hydrogen atom are well known, it is possible to calculate the first correction to the hydrogenoid spectrum, treating the $1/r_{23}^{1/2}$ term in Eq. (101) to first order in perturbation theory. The calculations are given in Appendix F, and we present here only the following result:

$$q_n^{(l)}R_* \underset{\alpha\to+\infty}{=} \frac{(\alpha/8)^{1/2}}{n+l}\left\{1-R_n^{(l)}\left[\frac{\pi(n+l)}{2\alpha}\right]^{1/2}+O\left(\frac{1}{\alpha}\right)\right\}, \quad (103)$$

where $R_n^{(l)}$ is a rational number given by

$$R_n^{(l)} = \frac{(n-1)!}{(n+2l)!}\sum_{k=0}^{n-1}\left[\frac{(2k)!}{(k!)^2}\right]^2 \times\frac{4^{-(n+2l+k)}}{(2k-1)^2}\frac{[2(2l+1+n-k)]!}{(n-1-k)!(2l+1+n-k)!}. \quad (104)$$

An interesting question is to know whether Eq. (103), which originates from the Born-Oppenheimer approximation, is still exact [50]. The discussion below Eq. (82) allows us to hope so. We shall present numerical evidence in Sec. V C that shows that this is indeed the case.

Another interesting aspect is to determine if the Born-Oppenheimer approximation, combined with a suitable semiclassical [Wentzel-Kramers-Brillouin (WKB) type] approximation, is able to determine exactly the global scale $q_{\rm global}^{(l)}$ in the large mass ratio limit. For a fixed angular momentum l, using the technique presented in Ref. [51] and setting here $E = -\hbar^2 Q^2/m$, we obtain the semiclassical quantization condition [52]

$$\int_{r_{\rm min}}^{r_{\rm max}} dr\left[\frac{\alpha}{2}\kappa^2(r)-\frac{(l+1/2)^2}{r^2}-Q^2\right]^{1/2} = (n-1/2)\pi, \quad (105)$$

where $r_{\rm min}$ and $r_{\rm max}$ are the lower and upper roots of the integrand and the quantum number n is any integer $\geqslant 1$. In the large n limit, Q tends to zero exponentially fast (this is the Efimovian part of the spectrum), so we can split the integral in Eq. (105) into two intervals, the interval $r_{\rm min} < r < r_{\rm int}$ where one can make the approximation $Q \simeq 0$ and the interval $r_{\rm int} < r < r_{\rm max}$ where the Born-Oppenheimer potential can be replaced by its asymptotic expression [Eq. (100)]. The intermediate value $r_{\rm int}$ simply has to satisfy $R_* \ll r_{\rm int} \ll |s_{\rm BO}|/\mathcal{Q}$, where $s_{\rm BO}$ is given by Eq. (76). The result then does not depend on the specific value of $r_{\rm int}$ and one finds an approximation for the Efimovian spectrum for $n \to +\infty$:

$$q_n^{(l)} R_* \approx \frac{2^{3/2}|s_{\rm BO}|(C-u_{\rm min})(1+C)}{C^2(1+\alpha)^{1/2}} e^{J_{\rm cl}} e^{-(n-1/2)\pi/|s_{\rm BO}|}, \tag{106}$$

where we have performed the change of variable $u = \kappa(r)r$ in the integral over r and one has $\alpha u_{\rm min}^2/2 = (l+1/2)^2$. The quantity $J_{\rm cl}$ is defined by the integral

$$J_{\rm cl} = -1 + \int_{u_{\rm min}}^{C} du \left[\left(\frac{2}{u} + \frac{1+e^u}{1-ue^u}\right) \times \left(\frac{u^2-u_{\rm min}^2}{C^2-u_{\rm min}^2}\right)^{1/2} - \frac{1}{C-u}\right]. \tag{107}$$

Whereas, as expected [52], this semiclassical result is disastrously bad for α close to the critical value $\alpha_c^{(l)}$ (it does not predict a finite $q_{\rm global}^{(l)}$ at the Efimovian threshold), it becomes increasingly accurate for increasing $\alpha - \alpha_c^{(l)}$. When compared to the exact numerical values of Fig. 4(a), we found that for $\alpha - \alpha_c^{(l)} > 8$, the error on $q_{\rm global}^{(l)}$ is already less than 10%. In the limit $\alpha \to +\infty$, the semiclassical result allows us to recover exactly the quantum result of Eq. (91), since $u_{\rm min} \to 0$ in that limit and $J_{\rm cl}$ then tends to J of Eq. (92). Keeping the first correction linear in $u_{\rm min}$ in the semiclassical result, we even get the refined estimate

$$q_{\rm global}^{(l)} R_* \underset{\alpha\to\infty}{=} 2(1+C)e^J\left[1 - \frac{\pi l}{|s_{\rm BO}|} + O(\ln\alpha/\alpha)\right]. \tag{108}$$

As this amounts to keeping the first $\alpha^{-1/2}$ term in a large α expansion, we can, again, hope that the Born-Oppenheimer approximation (combined to the semiclassical one) gives the exact result in Eq. (108) [53]. In Fig. 4(c) we have calculated $J_{\rm cl}$ and, hence, the semiclassical value of $q_{\rm global}^{(l)}$ numerically to show how it nicely interpolates between the large-α exact data of Fig. 4(a) (that still strongly depend on l) and the l-independent $\alpha \to +\infty$ limit of $q_{\rm global}^{(l)}$. Taking values of α as large as those in Fig. 4(c) is straightforward in the semiclassical formula, but it would be a numerical challenge for the exact expression of Eq. (71) (not to mention real experiments).

V. NUMERICAL SOLUTION FOR TRIMER STATES

In this section, we proceed with the direct numerical solution of the integral equation [Eq. (32)], looking for the allowed bound-state energies E for various values of the angular-momentum quantum number l. The motivation is to look for trimer states that are not predicted (or not faithfully predicted) by the analytical results of Sec. IV. First, in the presence of the Efimov effect (l odd, $\alpha > \alpha_c^{(l)}$), the analytical formula (84) is guaranteed to be asymptotically exact in the large quantum number $n \to +\infty$ limit, but the numerics can assess its accuracy for low values of n, $n \geqslant 1$ and can check whether $n = 1$ in Eq. (84) corresponds to the ground-state trimer for a given angular momentum. Second, it is, in principle, possible that the narrow Feshbach resonance model exhibits for $1/a = 0$ non-Efimovian trimers, which would appear for a mass ratio lower than $\alpha_c^{(l)}$. In single-channel models, with real interaction potentials, such few-body bound states were recently observed numerically [54,55] and their emergence was related to few-body resonances [55] that one may expect within the zero-range model when Eq. (34) has a real root s between 0 and 1 [27,56]. To be complete, let us mention that, for a *finite* and positive value of the scattering length, we expect that there exist a finite number of non-Efimovian $l = 1$ trimer states for mass ratios below the critical mass ratio $\alpha_c^{(l=1)}$, as shown in Ref. [57]. These interesting trimer states should have a vanishing energy right at the Feshbach resonance ($1/a = 0$) so they shall not show up in our numerical solution and their study is beyond the scope of the paper.

A. Optimized numerical method

The general method to numerically find the bound-state spectrum is to approximate the operator appearing in the momentum-space integral equation by a matrix, after discretization and truncation of the momentum k, and to perform a dichotomic or Newton search of the values of the energy $E < 0$ such that the resulting matrix has a zero eigenvalue. Here, we are dealing with the particular case of an infinitely narrow Feshbach resonance with an infinite scattering length, and a much more direct method can be used. The kernel in Eq. (32) does not involve any interaction length, and it exhibits $\hbar q$ as the only momentum scale, where the wave number q is the unknown since $E = -\hbar^2 q^2/(2\mu)$. We can thus rescale all wave numbers by q, setting $\check{k} = k/q, \check{K} = K/q$, and we introduce a reduced relative wave number

$$\check{q}_{\rm rel}(\check{k}) \equiv \frac{q_{\rm rel}(q\check{k})}{q} = \left[1 + \frac{1+2\alpha}{(1+\alpha)^2}\check{k}^2\right]^{1/2}. \tag{109}$$

For convenience, we also write the unknown function $f^{(l)}(k)$ as

$$f^{(l)}(k = q\check{k}) = \frac{\check{f}^{(l)}(\check{k})}{\check{k}\check{q}_{\rm rel}(\check{k})}, \tag{110}$$

where the denominator shall ensure that the resulting integral operator is Hermitian. After multiplication of Eq. (32) by $\check{k}/q_{\rm rel}(k)$, we obtain

$$-qR_*\check{f}^{(l)}(\check{k}) = \frac{1}{\check{q}_{\rm rel}(\check{k})}\check{f}^{(l)}(\check{k}) + \int_0^{+\infty} \frac{d\check{K}}{\pi} \frac{\check{f}^{(l)}(\check{K})}{\check{q}_{\rm rel}(\check{k})\check{q}_{\rm rel}(\check{K})} \times \int_{-1}^{1} du\, \frac{P_l(u)\check{k}\check{K}}{1+\check{k}^2+\check{K}^2+\frac{2\alpha}{1+\alpha}\check{k}\check{K}u}. \tag{111}$$

Remarkably, the dimensionless quantity $-qR_*$ is simply the solution of an eigenvalue problem for a fixed operator. After numerical discretization and truncation, one simply has to diagonalize a real symmetric matrix *once*, which is a well-mastered numerical problem, and each *negative* eigenvalue of that matrix will provide a numerical approximation of the quantity $-qR_*$ for the bound states. We expect the numerical truncation to be accurate if the maximal value $\check{k}_{\rm max}$ of $\check{k}$ in the numerical grid obeys, for each considered negative eigenvalue $-qR_*$,

$$q\check{k}_{\rm max}R_* \gg 1, \tag{112}$$

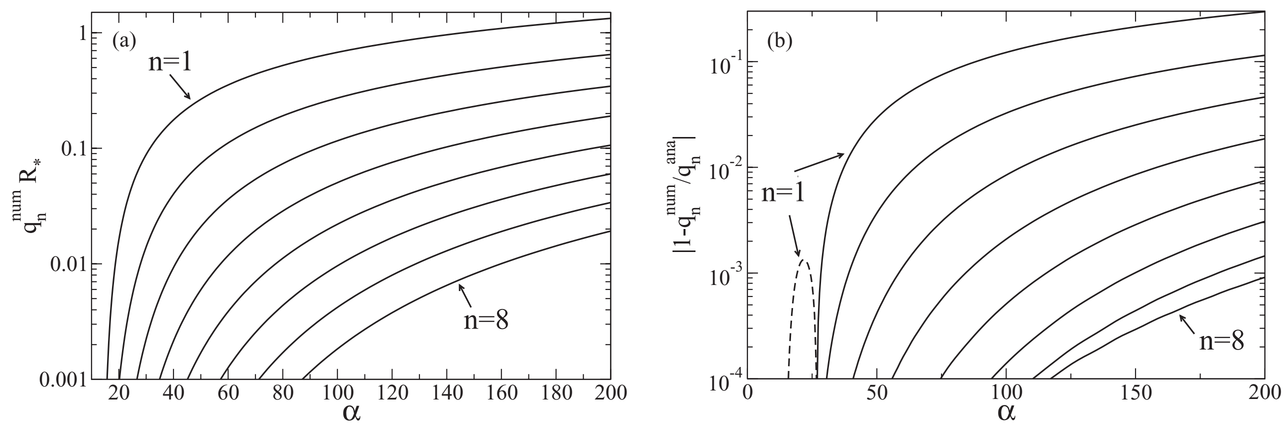

FIG. 6. Numerical study of the Efimovian part of the spectrum: For an angular momentum $l = 1$, quantities q_n (labeled in descending order) from $n = 1$ (ground trimer state) to $n = 8$, as functions of the mass ratio $\alpha = m/M$. We recall that the trimer energies are then $E_n = -\hbar^2 q_n^2/2\mu$. In (a) the numerical values are shown in log scale, restricting the figure to experimentally accessible values $qR_* > 10^{-3}$ (see text). In (b) the absolute value of the deviation from unity of the ratio of the numerical q_n to the analytical approximation (84). The solid (respectively dashed) lines correspond to numerical values of q_n larger (respectively smaller) than the analytical ones. For both (a) and (b), the vertical axis is in log scale, and the curves $n = 1$ to $n = 8$ are from top to bottom.

to ensure that the effective range term in the two-body scattering amplitude is well taken into account. For a given numerical diagonalization, the negative eigenvalues $-qR_*$ that are larger than $-1/\check{k}_{\max}$, thus, cannot be trusted. In these estimates, we have dropped, for simplicity, a possible dependence of the criteria on the mass ratio α [58].

In presence of the Efimov effect, the condition of Eq. (112) is quite severe, as qR_* may assume extremely small values. The way out is well known: One simply has to use a logarithmic scale, with the change of variable $x = \ln \check{k}, X = \ln \check{K}$. To keep the hermiticity of the operator, we reparametrize the unknown function

$$\check{f}^{(l)}(\check{k} = e^x) = \frac{\check{F}^{(l)}(x)}{e^{x/2}}. \tag{113}$$

Multiplying Eq. (111) by $\check{k}^{1/2}$ and performing these changes, we finally obtain the numerically useful form [59]:

$$\begin{aligned} -qR_*\check{F}^{(l)}(x) &= \frac{\check{F}^{(l)}(x)}{(1+e^{2x}\cos^2\nu)^{1/2}} \\ &+ \int_{-\infty}^{+\infty}\frac{dX}{\pi}\,\frac{\check{F}^{(l)}(X)}{[(1+e^{2x}\cos^2\nu)(1+e^{2X}\cos^2\nu)]^{1/2}} \\ &\times \int_{-1}^{1}du\,\frac{P_l(u)\,e^{3(x+X)/2}}{1+e^{2x}+e^{2X}+2ue^{x+X}\sin\nu} \end{aligned} \tag{114}$$

where we recall that $\nu = \arcsin[\alpha/(1+\alpha)]$; see Eq. (37). Another interesting feature of the form of Eq. (114), which it shares with Eq. (111), is that the kernel remains bounded at large momenta.

B. Efimovian results

We now present results obtained from a numerical solution of the eigenvalue problem of Eq. (114) for not-too-large values of the mass ratio so the trimer spectrum does not exhibit the hydrogenoid character predicted in Sec. IV C. In the numerics, we took for the variable $x = \ln \check{k}$ a discretization with a constant step $dx = 0.09$ over an interval from $x_{\min} = \ln(10^{-2})$ to $x_{\max} = \ln(10^{15})$. We explored the interval of mass ratio $\alpha = m/M$ from the small value $1/200$ to the large value 200.

We, first, explored the case of even angular momenta. According to the zero-range theory, numerical observation of bound states in that case would reveal non-Efimovian trimers. We went up to an angular momentum $l = 12$ without finding any bound state: The minimal eigenvalues $-qR_*$ found numerically were positive and of the order of 10^{-15} or larger. We then explored odd angular momenta, looking for non-Efimovian bound states for a mass ratio $\alpha < \alpha_c^{(l)}$ (and $\alpha < 200$). We went up to $l = 13$ without finding any.

At this stage, exploration of Efimovian physics remains. The numerical results for the most bound trimer states are shown for $l = 1$ in Fig. 6. In Fig. 6(a) we directly show the obtained values of qR_* as functions of the mass ratio α, obviously in log scale for the vertical axis. This is useful to estimate which trimer states may be accessed in an experiment. An experimental limitation is that the scattering length a is not infinite, which will suppress the too-weakly bound trimers, that is, the trimer states with a too-small value of q. According to Eq. (26) we see that if $1/|a| \ll q$, the term $1/a$ is small as compared to the term $q_{\text{rel}}(k)$ for all values of k, so the assumption $1/a = 0$ should be a good approximation. Assuming that producing in a controlled way a scattering length larger than 100 μm (in absolute value) becomes unrealistic, in particular for a narrow Feshbach resonance, we thus take

$$|a^{\text{expt}}| \lesssim 100\,\mu\text{m} \tag{115}$$

and we impose $q > 10/|a| \approx 10/(100\ \mu\text{m})$. Since R_* should be much larger than the typical van der Waals length (typically of a few nanometers), we take $R_* > 10$ nm, so $qR_* > 10^{-3}$; hence, the interval of values on the vertical axis in Fig. 6(a) [60].

In Fig. 6(b), we show the ratios of the numerical values of qR_* to the values obtained from the approximation of Eq. (84) as functions of the mass ratio. The numerical values are numbered as $n = 1$ (ground-state trimer state), $n = 2,3,\ldots$, for q in descending order (that is, in ascending order of the energies $E_n = -\hbar^2 q_n^2/2\mu$). The numerical q_n are then each divided by the approximate q_n of Eq. (84). For α close to $\alpha_c^{(l=1)}$, for example, $\alpha \leqslant 20$, it is found that the ratio of numerical to analytical values of the q's is extremely close to unity: For the ground trimer $n = 1$, the deviation is less than 10^{-3}, and for $n = 2$ and $n = 3$ it fluctuates between $\pm 10^{-5}$, which is probably due to numerical errors. Similar results are obtained for larger odd values of l (not shown).

We have, thus, numerically obtained the important result that the quantum number $n = 1$ in the analytical formula (84) indeed corresponds to the ground trimer state (within each subspace of fixed l). For not-too-large $\alpha - \alpha_c^{(l)}$ (away from the hydrogenoid regime), the binding energy of the ground trimer state thus does not correspond to the naive expectation $\approx \hbar^2/(\mu R_*^2)$; it contains an extra factor $\exp(-2\pi/|s_l|)$ that can be tiny. There is numerical evidence that this also holds for three bosons resonantly interacting on a narrow Feshbach resonance [61]; the impossibility in the bosonic case to connect the spectrum continuously to a $S_l = 0$ limit (and to study the variation of the three-body parameter in that limit), however, makes the statement more subjective than in the present fermionic case.

To be complete, we have also calculated numerically the eigenvectors $x \to \check{F}^{(l)}(x)$ corresponding to the eigenvalues $-q_n^{(l)} R_*$ in the case $l = 1$ for $\alpha = 14$. According to Eqs. (110) and (113), one has $\check{F}^{(l)}(x) = e^{3x/2}(1 + e^{2x}\cos^2\nu)^{1/2} f^{(l)}(qe^x)$. For $k/Q \ll 1$, that is, $e^x \cos\nu \ll 1$ since $Q = q/\cos\nu$, we found that $\check{F}^{(l=1)}(x) \propto e^{5x/2}$ as deduced from Eq. (52) (multiplied by i). For $kR_* \cos\nu \gg 1$, that is, $e^x \cos\nu \gg e^{\pi n/|s_1|}$, where $s_1 = iS_1$ is the purely imaginary Efimov exponent for $l = 1$, we found that $\check{F}^{(l=1)}(x) \propto e^{-5x/2}$, as predicted by Ref. [41]. Finally, in the crucial intermediate region $q/\cos\nu < k < 1/(R_* \cos\nu)$, which corresponds to the matching interval of the $(E < 0, R_* = 0)$ and $(E = 0, R_* > 0)$ analytical solutions, see Fig. 3, we compared the numerics to the analytical result deduced from Eq. (53) (multiplied by i) as follows:

$$\check{F}^{(l=1)}(x) \propto e^{x/2} \sin[|s_1|(x - x_0)], \tag{116}$$

where $x_0 = (\arctan|s_1|)/|s_1| - \ln(2\cos\nu)$. From the numerics, see Fig. 7, we found that $x \to e^{-x/2}\check{F}^{(l=1)}(x)$ indeed exhibits half an oscillation of the sinus for the ground trimer $n = 1$ (the function remains positive everywhere), and a full oscillation of the sinus for the first excited trimer $n = 2$ (the function changes sign once).

These nodal properties were expected from the fact noted in Ref. [59] that the matrix elements of the kernel in Eq. (114) are strictly negative for l odd for all x and X, whereas the diagonal element is strictly positive for all x. From a standard variational argument, that formulates Eq. (114) in terms of the extremalization of an "energy" functional for a fixed norm, and that compares the "energy" of $x \to \check{F}^{(l)}(x)$ to the one of $x \to |\check{F}^{(l)}(x)|$, we conclude that the function $\check{F}^{(l)}(x)$ for the ground trimer state has a constant sign. As the other modes

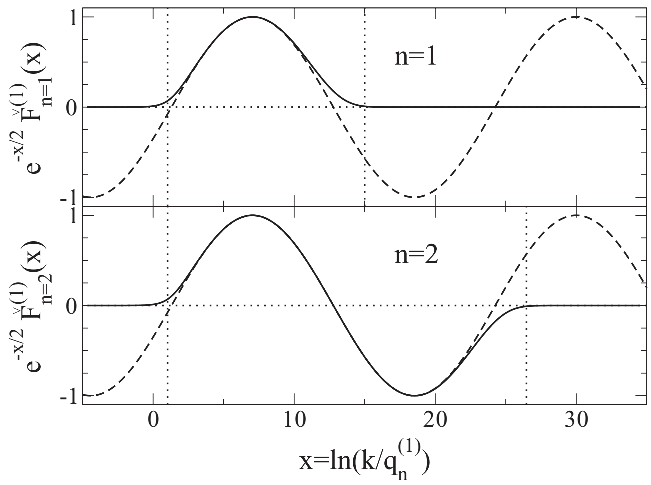

FIG. 7. For $l = 1$ and a mass ratio $\alpha = 14$, the ground eigenvector ($n = 1$) and first excited eigenvector ($n = 2$) of the eigenvalue problem [Eq. (114)], corresponding to the ground and first excited trimer states. (Solid lines) Numerical results. (Dashed lines) Analytical form [Eq. (116)], meaningful over the matching interval $1/\cos\nu < k/q < 1/(qR_* \cos\nu)$ whose meaning is explained in Fig. 3 and whose borders are indicated by the vertical dotted lines. The expression of $D(\mathbf{k})$ in terms of $\check{F}^{(1)}(x)$ and $Y_1^0(\mathbf{k})$ can be obtained from the text, with $x = \ln(k/q)$. An overall factor $\exp(-x/2)$ was applied to $\check{F}^{(1)}(x)$ for convenience, and the resulting functions are normalized to the maximal value of unity.

have to be orthogonal to the ground mode, this shows that the ground trimer state is not degenerate and that the excited trimer states have a sign-changing function $\check{F}^{(l)}(x)$. We have, thus, reached a fully consistent picture of the fact that $n = 1$ in Eq. (84) is indeed the ground trimer state.

C. Hydrogenoid results

We now explore numerically the trimer spectrum for extremely large values of the mass ratio α. In this limit, the low-energy trimers are no longer expected to be Efimovian: According to the Born-Oppenheimer approach of Sec. IV C, the spectrum for fixed values of the quantum numbers n and l becomes hydrogenoid for $\alpha \to +\infty$. To test the asymptotic analytical formula (103), we plot in Fig. 8 the ratio of the wave number $q_n^{(l)}$ [such that $E_n^{(l)} = -\hbar^2[q_n^{(l)}]^2/(2\mu)$] to the asymptotic prediction [Eq. (102)] as a function of $1/\alpha^{1/2}$ for $l = 1$ and a few values of n (we recall that $n = 1$ labels the ground trimer state for fixed l). The prediction Eq. (103) then corresponds to straight lines, and we indeed observe that the numerical results approach these straight lines for diverging α. This suggests that Eq. (103), obtained in the Born-Oppenheimer approximation, is actually asymptotically exact. As expected, for increasing n, the trimers become spatially more extended, so a larger value of α is required to make them hydrogenoid.

Some considered values of α in Fig. 8 are extremely large (up to 10^6). This cannot be realized with atoms, and, as such, a large mass ratio does not exist in the periodic table. Using an optical lattice as suggested in Ref. [62] is possible if the trimer states have a spatial extension much larger than the lattice spacing. This may require unrealistically large values

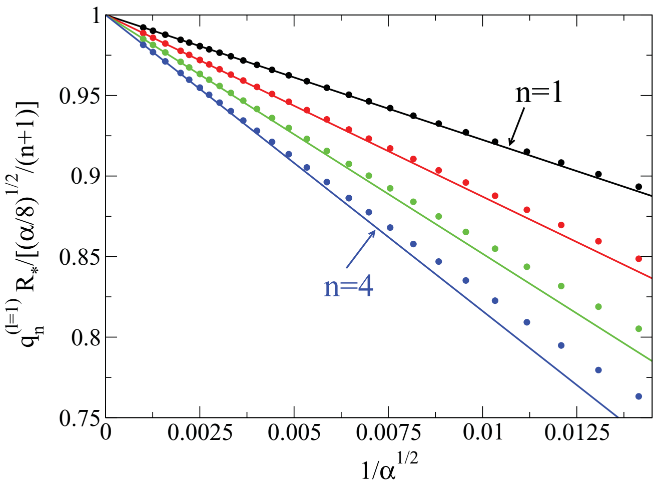

FIG. 8. (Color online) Numerical study of the hydrogenoid part of the spectrum: For an angular momentum $l = 1$, wave numbers $q_n^{(l)}$ for $n = 1$ (ground trimer state), $n = 2$, $n = 3$, and $n = 4$ (from top to bottom), divided by the hydrogenoid asymptotic Born-Oppenheimer prediction [Eq. (102)], as functions of $1/\alpha^{1/2}$. (Solid circles) Numerical results. (Straight lines) Asymptotic result [Eq. (103)], including the first deviation of the Born-Oppenheimer potential from the Coulomb form at short range. The color code is as follows: black for $n = 1$, red for $n = 2$, green for $n = 3$, and blue for $n = 4$.

of R_*. A futuristic alternative is to replace the fermionic atoms by large and round molecules that are cooled to their internal (vibrational and rotational) ground state, that have a vanishing total angular momentum in that ground state, that may be in the class of fullerenes [63], and that would exhibit a narrow Feshbach resonance with the extra atom.

VI. CONCLUSION

We have performed a detailed study of the quantum three-body problem of two same-spin-state fermions of mass m interacting in free space with a distinguishable particle of mass M on an infinitely narrow Feshbach resonance, with a focus of the three-body bound states (trimer states) of that system. The interaction was assumed to be tuned right on resonance, with an infinite s-wave scattering length a, which makes it possible to obtain analytical results, since the only length scale left in the problem is the so-called Feshbach length R_* [7]. The assumption $1/a = 0$ also ensures that there are no two-body bound states. This three-body problem, however, remains rich, richer than,e.g., the problem of three resonantly interacting bosons on a narrow Feshbach resonance [7,11,12], because there is a tunable parameter left, which is the mass ratio $\alpha = m/M$ of a fermion to the extra particle. The existence of this tunable parameter raises the following three fundamental questions on the trimer states within each sector of *fixed* total angular momentum l.

First, does this system support trimer states for a mass ratio α *smaller* than the minimal mass ratio α_c required to activate the Efimov effect [4]? Such non-Efimovian trimer states may indeed emerge from three-body resonances recently discovered numerically for a different interaction model [54,55], with an Efimov exponent s having a *real* value between 0 and 1 [27,56]. For the narrow Feshbach resonance, our numerical answer to this question is negative.

Second, how does the Efimov trimer spectrum emerge when the mass ratio α is varied across the critical value α_c (necessarily for l odd)? This is an intriguing question, because there is no trimer state for $\alpha < \alpha_c$ (for fixed l) and there is an infinite number of trimer states for $\alpha > \alpha_c$. We found that, for α tending to α_c from above, the *whole* trimer spectrum, including the ground trimer state (and not simply the trimer states with large quantum number n) forms a geometric sequence. This, of course, cannot be deduced from general zero-range Efimov's theory, which guarantees the geometric nature of the spectrum only in the asymptotic region of large quantum number n and cannot say anything about, e.g., the model-dependent ground trimer state. We have also shown that the global energy scale E_{global} in that spectrum has a finite and nonzero limit for $\alpha \to \alpha_c$. This simply means that, at the Efimovian threshold, the energy of the ground-state trimer vanishes as $E_{\text{global}} \exp(-2\pi/|s|)$, the energy of the first excited trimer vanishes as $E_{\text{global}} \exp(-4\pi/|s|)$, and so on, where the modulus of the purely imaginary Efimov exponent s vanishes as the square root of $\alpha - \alpha_c$. This constitutes a complete picture of the emergence of the Efimovian trimer states when the mass ratio is varied across α_c. The dependence of E_{global} on the mass ratio α and on the angular momentum l was further studied analytically by use of an efficient expression of E_{global} in terms of an asymptotic series; see Eqs. (85) and (87).

Third, what is the nature of the most bound trimer states, for example, the ground state, when the mass ratio α becomes significantly larger than the critical value α_c? As already mentioned, Efimov's theory cannot answer this model-dependent question. For the narrow Feshbach resonance, we found that the low-energy part of the spectrum becomes asymptotically equivalent to a hydrogenoid spectrum for a diverging mass ratio, that is, scaling as $E_0/(n + l)^2$, where $n \geqslant 1$, l is odd and $E_0 = -m\hbar^2/(4MR_*)^2$, and we calculated the first deviation from this hydrogenoid spectrum for a finite α. As the hydrogenoid nature asymptotically takes over the Efimovian nature of the trimer spectrum for $\alpha \to +\infty$ (except in a vicinity of the $E = 0$ accumulation point where the spectrum remains geometric), in a continuous way when the mass ratio is varied, this constitutes a crossover from an Efimovian to a hydrogenoid spectrum.

We have also discussed to what extent all these predictions for the (2 + 1)-fermion problem on a narrow Feshbach resonance may be addressed experimentally with cold atoms, the variation of the mass ratio being obtained by combining the discrete tuning provided by the choice of appropriate species for the fermions and the extra particle, with an additional continuous fine tuning of the effective mass with an optical lattice [62]. Reaching the large mass ratios required to observe the hydrogenoid part of the spectrum is challenging, except for the futuristic alternative of replacing the fermionic atoms with massive and round molecules. On the contrary, the Efimovian effect in our system may be reachable experimentally for angular momentum $l = 1$, where the critical mass ratio is only $\alpha_c \simeq 13.607$, provided that the energy ratio $\exp(2\pi/|s|)$ is not too large, that is, the mass ratio is far enough from the critical value α_c where $|s| = 0$. From the bound of Eq. (115) on the achievable s-wave scattering length a with a magnetic Feshbach resonance, the ground-state trimer is directly observable for $\alpha > 15$, whereas directly observing at least *two* Efimovian trimer states, to check the geometric nature of the spectrum, requires $\alpha > 20$. On a Feshbach resonance as narrow as the one of ^{6}Li with ^{40}K, however, the bound of Eq. (115) is probably too optimistic, if one does not implement a magnetic field stabilization of metrologic quality [60].

ACKNOWLEDGMENTS

We warmly thank L. Pricoupenko and C. Mora for fruitful discussions at an early stage of this work, A. Sinatra for useful comments on the manuscript, and F. Werner for pointing out useful references.

APPENDIX A: ZERO-RANGE SOLUTION IN POSITION SPACE

In the case $R_* = 0$, our three-body problem reduces to the zero-range infinite scattering length problem that Efimov solved in real space [4] with the ansatz for the three-body wave function:

$$\psi(\mathbf{r}_1,\mathbf{r}_2,\mathbf{r}_3) = \frac{F(R)}{R^2}\left[\frac{\varphi(\alpha_{21})}{\sin(2\alpha_{21})}Y_l^{m_l}\left(\mathbf{r}_3 - \frac{\alpha\mathbf{r}_2+\mathbf{r}_1}{1+\alpha}\right) - \frac{\varphi(\alpha_{31})}{\sin(2\alpha_{31})}Y_l^{m_l}\left(\mathbf{r}_2 - \frac{\alpha\mathbf{r}_3+\mathbf{r}_1}{1+\alpha}\right)\right]. \quad \text{(A1)}$$

This contains two *a priori* unknown functions of single variables, F and φ. The various variables in this ansatz naturally appear in appropriately normalized Jacobi coordinates. Using, e.g., the convention of Appendix 3 in Ref. [29] (except for a permutation of the indices), and taking as in Eq. (13) particle 1 as the extra particle of mass $m_1 = M$, and particles 2 and 3 as the fermions of mass $m_2 = m_3 = m$, we define the unnormalized Jacobi coordinates $\mathbf{y}_1 = \mathbf{r}_3 - (m\mathbf{r}_2 + M\mathbf{r}_1)/(m+M)$ and $\mathbf{y}_2 = \mathbf{r}_1 - \mathbf{r}_2$, the generalized reduced masses $\mu_1^{-1} = m^{-1} + (m+M)^{-1}$ and $\mu_2^{-1} = M^{-1} + m^{-1}$, and the hyperradius $R \geqslant 0$ such that $\bar{m}R^2 = \sum_{i=1}^3 m_i(\mathbf{r}_i - \mathbf{C})^2$, where $\bar{m}$ is an arbitrary unit of mass and $\mathbf{C}$ is the center-of-mass position of the three particles. The conveniently normalized Jacobi coordinates then are $\mathbf{u}_i = (\mu_i/\bar{m})^{1/2}\mathbf{y}_i$ with $i = 1,2$, so $R^2 = u_1^2 + u_2^2$. This also puts Schrödinger's equation in a reduced form,

$$\sum_{i=1}^{3} -\frac{\hbar^2}{2m_i}\Delta_{\mathbf{r}_i} = -\frac{\hbar^2}{2(2m+M)}\Delta_{\mathbf{C}} + \sum_{i=1}^{2} -\frac{\hbar^2}{2\bar{m}}\Delta_{\mathbf{u}_i}. \quad \text{(A2)}$$

The angles α_{21} and α_{31} belong to the interval $[0,\pi/2]$. The clever choice is $\tan\alpha_{21} = u_2/u_1$ and the similar formula for α_{31} obtained by exchanging the role of particles 2 and 3. Geometrically, this amounts to introducing polar coordinates (R,α_{21}) in the plane (u_1,u_2). Explicitly, this gives

$$\tan\alpha_{21} = \frac{|\mathbf{r}_1 - \mathbf{r}_2|\cos\nu}{|\mathbf{r}_3 - (\alpha\mathbf{r}_2 + \mathbf{r}_1)/(1+\alpha)|} \quad \text{(A3)}$$

$$\tan\alpha_{31} = \frac{|\mathbf{r}_1 - \mathbf{r}_3|\cos\nu}{|\mathbf{r}_2 - (\alpha\mathbf{r}_3 + \mathbf{r}_1)/(1+\alpha)|} \quad \text{(A4)}$$

where $\cos\nu$ is given by Eq. (38). Since the second (Faddeev) component in Eq. (A1) is deduced from the first one by a minus sign and the exchange of particles 2 and 3, which ensures the fermionic antisymmetry of ψ, it suffices to calculate the action of $\Delta_{\mathbf{u}_1} + \Delta_{\mathbf{u}_2}$ on the first component. This is quite simple in spherical coordinates, since R and α_{21} depend only on the moduli u_1 and u_2, and the factor involving the spherical harmonic function is simply $Y_l^{m_l}(\mathbf{u}_1)$. Thanks to the factor $R^2\sin(2\alpha_{21}) = 2u_1u_2$ in the denominator, one is left with the operator $\partial_{u_1}^2 + \partial_{u_2}^2$, that is, the Laplacian in the plane (u_1,u_2), which has a simple expression in the polar coordinates (R,α_{21}). One finally finds that the ansatz [Eq. (A1)] separated in hyperspherical coordinates solves Schrödinger's equation if φ solves the eigenvalue problem

$$-\varphi''(\alpha_{21}) + \frac{l(l+1)}{\cos^2\alpha_{21}}\varphi(\alpha_{21}) = s^2\varphi(\alpha_{21}), \quad \text{(A5)}$$

where s is *a priori* unknown, but the general theory of, e.g., Sec. 3.3 in Ref. [29] guarantees that it coincides with s defined in Fourier space by Eq. (33). As a consequence, the R dependence of the ansatz also separates and the hyper-radial function $F(R)$ is found to solve a Schrödinger equation for a fictitious particle in two dimensions experiencing an effective $1/R^2$ potential:

$$EF(R) = -\frac{\hbar^2}{2\bar{m}}\left[F''(R) + \frac{1}{R}F'(R)\right] + \frac{\hbar^2 s^2}{2\bar{m}R^2}F(R). \quad \text{(A6)}$$

The Efimov effect appears for $s^2 < 0$.

To determine the eigenvalue s^2, one needs to specify the boundary conditions for φ. For $u_1 \to 0$, ψ, in general, does not diverge. Since $\sin(2\alpha_{21})$ vanishes in the denominator, this imposes

$$\varphi(\pi/2) = 0. \quad \text{(A7)}$$

For $u_2 \to 0$, on the contrary, ψ diverges. More precisely, the Bethe-Peierls contact conditions for an infinite scattering length impose that, when particles 1 and 2 approach each other for a fixed position of their center of mass $\mathbf{C}_{12}$, that is, $\mathbf{r}_2 = \mathbf{C}_{12} - \mathbf{r}/(1+\alpha)$ and $\mathbf{r}_1 = \mathbf{C}_{12} + \alpha\mathbf{r}/(1+\alpha)$ with $r \to 0$, ψ should behave as $A/r + O(r)$ where A depends on $\mathbf{C}_{12} - \mathbf{r}_3$. In other words, there should be no nonzero contribution behaving as r^0. To calculate the r^0 contribution from the first Faddeev component, one has to expand $\varphi(\alpha_{21})$ to first order in α_{21}. In the second Faddeev component one can directly set $\mathbf{r} = 0$, that is, $\mathbf{r}_1 = \mathbf{r}_2 = \mathbf{C}_{12}$. From the angular representation (37) for the mass ratio, we find $\arctan[(1+2\alpha)^{1/2}/\alpha] = \frac{\pi}{2} - \nu$ and

$$\frac{1}{2}\varphi'(0) - (-1)^l\frac{\varphi\left(\frac{\pi}{2} - \nu\right)}{\sin(2\nu)} = 0. \quad \text{(A8)}$$

To try to recover the function $\Lambda_l(s)$, we heuristically multiply this condition by $2\cos\nu/\varphi'(0)$ to pull out a first additive term as in Eq. (42):

$$\Lambda_l(s) \stackrel{?}{=} \cos\nu - (-1)^l\frac{\varphi\left(\frac{\pi}{2} - \nu\right)}{\varphi'(0)\sin\nu}. \quad \text{(A9)}$$

Note that Eq. (A5) is independent of the mass ratio, and it occurs in the problem of three spin-1/2 (same mass) fermions and even in the case of three bosons. The solution of Eq. (A5) obeying Eq. (A7) was given in these contexts in Ref. [32] in terms of a hypergeometric function. Reusing this solution

$$\varphi(\alpha_{21}) = \cos^{l+1}\alpha_{21} \times {}_2F_1\left(\frac{l+1+s}{2},\frac{l+1-s}{2},l+\frac{3}{2};\cos^2\alpha_{21}\right) \tag{A10}$$

leads to Eq. (44), which was checked numerically to coincide with Eq. (42), so the question mark can be removed in Eq. (A9). For completeness, we note that still another form of $\varphi(\alpha_{21})$, in terms of a finite sum, was given in Ref. [30].

APPENDIX B: EFIMOVIAN SPECTRUM GLOBAL SCALE AT THRESHOLD

At fixed angular momentum l, we evaluate the global scale $q_{\rm global}^{(l)}$ in the limit $\alpha \to \alpha_c^{(l)}$. Since $s_l = iS_l$, $S_l > 0$, vanishes in that limit, we can simply expand the complex number Z_l up to order S_l, neglecting terms $O(S_l^2)$. The most difficult part is the bit $iS_l\, C_l(-S_l)$, which we rewrite using Eq. (71), $\Gamma(2iS_l) = \Gamma(1+2iS_l)/(2iS_l)$, as follows:

$$iS_l\, C_l(-S_l) = \frac{\Gamma(1+2iS_l)\Gamma(1-iv_0-iS_l)}{2\Gamma(1)\Gamma(-iv_0+iS_l)} \times \prod_{n\in\mathbb{N}^*}\frac{\Gamma(-iu_n+iS_l)}{\Gamma(1-iu_n-iS_l)}\,\frac{\Gamma(1-iv_n-iS_l)}{\Gamma(-iv_n+iS_l)}. \tag{B1}$$

We, first, need to figure out to which order the roots u_n depend on $u_0 = S_l$ (remember that the v_n's do not depend on the mass ratio). To zeroth order, right on the critical mass ratio, $u_n = u_n^c$ by definition. Making apparent the dependence of the function Λ_l with α, one has

$$\Lambda_l(iu_n;\alpha) = 0. \tag{B2}$$

It is clear on Eq. (41) that Λ_l is a regular function of α, so $\Lambda_l(s;\alpha)$ around $\alpha_c^{(l)}$ varies to first order in $\alpha-\alpha_c^{(l)}$ and (B2) simplifies to

$$\Lambda_l\big(iu_n;\alpha_c^{(l)}\big) = O\big(\alpha-\alpha_c^{(l)}\big). \tag{B3}$$

We also note that $\Lambda_l(s;\alpha)$ is an even function of s. For $n=0$, $u_0 = S_l$ and $u_0^c = 0$; since 0 is a double root of $s \to \Lambda_l(s;\alpha_c^{(l)})$, one has to expand Eq. (B3) to second order in $u_n - u_n^c$ to get the leading contribution, and S_l^2 varies linearly in $\alpha-\alpha_c^{(l)}$, as expected. For $n>0$, $u_n^c \neq 0$ and iu_n^c is a *simple* root of $s \to \Lambda_l(s;\alpha_c^{(l)})$, and one has to expand Eq. (B3) to first order in $u_n - u_n^c$ to get the leading contribution so

$$u_n - u_n^c = O\big(\alpha-\alpha_c^{(l)}\big) = O\big(S_l^2\big) \quad \text{for } n>0. \tag{B4}$$

To first order in S_l, we can thus replace the u_n's in Eq. (B1) by their values u_n^c at threshold (for $n>0$).

The last step is to expand the Γ functions in Eq. (B1) to first order in S_l. For any real positive number $x>0$, one has

$$\frac{\Gamma(x+iS_l)}{\Gamma(x)} = 1 + iS_l\psi(x) + O\big(S_l^2\big), \tag{B5}$$

where $\psi(z) = \Gamma'(z)/\Gamma(z)$ is the digamma function. One has, in particular, $\psi(1) = -\gamma$, where $\gamma = 0.577\,215\,664\,9\ldots$ is Euler's constant, see, e.g., relation 8.362(1) in Ref. [31]. We recall that, by definition, $-iu_n$ for $n>0$ and $-iv_n$ for $n \geqslant 0$ are real positive. Finally, the product over n in Eq. (86) may be written as $\Gamma(l+1-iS_l)/\Gamma(1-iS_l)$ and expanded with the same technique. All this leads to Eq. (88).

To reveal the convergence of the series in Eq. (88), it is useful to introduce the function $\Phi(x) = \psi(x)+\psi(x+1) - 2\ln x$. Then $\Phi(x) = O(1/x^2)$ for $x \to +\infty$ since $\psi(x+1) = \ln x + \frac{1}{2x} + O(1/x^2)$ according to relation 8.344 in Ref. [31]. Expressing $\psi(x)+\psi(x+1)$ as $\Phi(x) + 2\ln x$ for $x = -iu_n^c$ and $x = -iv_n$, and collecting all the logarithmic contributions as the logarithm of the product $\prod_{n\geqslant 1}\frac{(u_n^c)^2}{v_n^2}$, which one can relate to the curvature in $s=0$ of the function $\Lambda_l(s;\alpha)$ thanks to Eq. (70), one obtains

$$\frac{\theta_l}{|s_l|} \underset{S_l\to 0^+}{\to} -\psi(l+1) + 3\psi(1) - \psi(-iv_0) - \psi(1-iv_0) + \ln\left[\frac{v_0^2}{2\cos\nu}\partial_s^2\Lambda_l(0;\alpha_c^{(l)})\right] + \sum_{n=1}^{+\infty}\left[\Phi\big(-iu_n^c\big) - \Phi(-iv_n)\right]. \tag{B6}$$

As one expects that $u_n/v_n \to 1$ for $n \to +\infty$, with $v_n = i(2n+l+1)$, from the supposed convergence of the infinite product in Eq. (70), the sum in Eq. (B6) is convergent.

In practice, it is found that the sum over $n \geqslant 1$ in Eq. (B6) is so rapidly convergent that it gives a very small contribution to the result. A useful, easy-to-evaluate approximation is, thus,

$$\lim_{\alpha\to\alpha_c^{(l)}} q_{\rm global}^{(l)} \simeq -\frac{(l+1)^2}{R_*\cos\nu}\, e^{-2\psi(l+1)-\psi(l+2)+3\psi(1)}\partial_s^2\Lambda_l(0;\alpha_c^{(l)}). \tag{B7}$$

The relative error introduced by this approximation is, at most, $\simeq 5\times 10^{-4}$ for the values of l (from 1 to 11) that we have considered. Note that the approximation of Eq. (B7) is equivalent to neglect all terms with $k \geqslant 1$ in Eq. (87) and to take the limit $\alpha \to \alpha_c^{(l)}$.

APPENDIX C: ALTERNATIVE REPRESENTATIONS OF THE FUNCTION $C_l(S)$

To determine $q_{\rm global}^{(l)}$ of Eq. (85), that is, the phase θ_l of the complex number Z_l in Eq. (86), in the large l limit for fixed $\alpha-\alpha_c^{(l)}$ or in the large α limit for l fixed, the infinite product form [Eq. (71)] for the function $C_l(S)$ is inappropriate, even numerically. We construct here more efficient representations, in the same manner that led to Eq. (B6). Remarkably, the last form that we construct does not rely on the roots and poles of the function Λ_l.

We split the function $C_l(S)$ of Eq. (71) in parts whose phase is easy(difficult) to evaluate. Since $-iu_n$ is real for $n>0$, and S is real, using $\Gamma(z)^* = \Gamma(z^*)$ we rewrite the factors of Eq. (71) as

$$\frac{\Gamma(-iS-iu_n)}{\Gamma(1+iS-iu_n)} = \frac{\Gamma(-iS-iu_n)\Gamma(1-iS-iu_n)}{|\Gamma(1+iS-iu_n)|^2}. \tag{C1}$$

A similar rewriting can be performed on the factors involving $-iv_n$, $n>0$, so, apart from an infinite product that is real positive and does not contribute to the phase of $C_l(S)$, we identify a hard part $D_l(S)$ that is the product of factors of the form $\Gamma(z)\Gamma(z+1)$, with $z=-iu_n-iS$ in the numerator and $z=-iv_n-iS$ in the denominator. We then set

$$\Psi(z)=\frac{\Gamma(z)\Gamma(z+1)}{2\pi e^{2f(z)}} \quad \text{with} \quad f(z)=z\ln z-z. \tag{C2}$$

Here we have the case where $\mathrm{Re}\, z>0$ so the branch cut of the logarithm (on the real negative axis) and the poles of $\Gamma(z)$ are out of reach. Then

$$D_l(S)=e^{\Sigma_l(S)}\prod_{n\in\mathbb{N}^*}\frac{\Psi(-iu_n-iS)}{\Psi(-iv_n-iS)} \tag{C3}$$

with

$$\Sigma_l(S)=2\sum_{n\in\mathbb{N}^*}[f(-iu_n-iS)-f(-iv_n-iS)]. \tag{C4}$$

According to the relation 8.344 in Ref. [31], $\Psi(z)=1+O(1/z)$ at large $|z|$ so one expects that the infinite product in Eq. (C3) converges more rapidly than the original form [Eq. (71)]. Furthermore, only the imaginary part of $\Sigma_l(S)$ is required, and it can be expressed as the integral

$$\mathrm{Im}\,\Sigma_l(S)=-\int_0^S dS'\,R_l(S') \tag{C5}$$

with

$$R_l(S)=\ln\left[\frac{\Lambda_l(iS)}{\cos\nu}\,\frac{S^2+(l+1)^2}{S^2-S_l^2}\right]. \tag{C6}$$

Equation (C5) holds for $S=0$, since $-iu_n$ and $-iv_n$ are all real positive for $n>0$. To check that it holds at nonzero S, one takes the derivative of Eq. (C5) with respect to S, using $f'(z)=\ln z$ and $f(z)^*=f(z^*)$. One then recognizes the function $\Lambda_l(iS)$ from its Weierstrass representation [Eq. (70)], also using $v_0=i(l+1)$ and $u_0=S_l$.

It is possible to go further and to express the phase of the infinite product in Eq. (C3) in terms of derivatives of the function $R_l(S)$. Relation 8.344 in Ref. [31] indeed gives Stirling's representation of $\ln\Psi(z)$ as an *asymptotic* series in $1/z$, and one also has the kth derivative for $k\geqslant 1$,

$$\frac{d^k}{dS^k}[\ln(-iu_n-iS)]=\frac{-i^k(k-1)!}{(-iu_n-iS)^k}, \tag{C7}$$

and similar relations obtained by taking the complex conjugate or by replacing u_n with v_n. Finally, $D_l(S)=|D_l(S)|\exp[i\varphi_l(S)]$ with

$$\varphi_l(S)=-\int_0^S dS'\,R_l(S')-\sum_{k\geqslant 1}\frac{(-1)^k B_{2k}}{(2k)!}R_l^{(2k-1)}(S), \tag{C8}$$

where the B_{2k} are the Bernoulli numbers and $R_l^{(2k-1)}$ stands for the $(2k-1)^{\text{th}}$ derivative of the function $R_l(S)$. The useful statement is then that

$$\frac{C_l(-S_l)e^{i\varphi_l(S_l)}}{\Gamma(2iS_l)\Gamma(l+1-iS_l)\Gamma(l+2-iS_l)} \text{ is real positive} \tag{C9}$$

where we used the fact that $R_l(S)$ is an even function of S and, thus, $\varphi_l(S)$ an odd function of S. Minor transformations then lead to Eq. (87). In short, these results originate from the lemma: For any $x>0$ and S real,

$$\begin{aligned}\mathrm{Im}[\ln\Gamma(x-iS)+\ln\Gamma(x+1-iS)]&\\ =-\int_0^S dS'\ln(x^2+S'^2)&\\ -\sum_{k\geqslant 1}(-1)^k\frac{B_{2k}}{(2k)!}\frac{d^{2k-1}}{dS^{2k-1}}\ln(x^2+S^2),&\end{aligned} \tag{C10}$$

where, here again, the series is only asymptotic.

APPENDIX D: EFIMOVIAN SPECTRUM GLOBAL SCALE AT LARGE ANGULAR MOMENTA

As we show here, asymptotically exact expressions of $q_{\text{global}}^{(l)}$ for a diverging angular momentum l can be obtained analytically. This requires an asymptotic determination of the function $\Lambda_l(iS)$. To this end, the most convenient starting point is the expression for Λ_l in Eq. (44). Since $\cos\nu$ tends to zero for $\alpha>\alpha_c^{(l)}$ in the large l limit, we rewrite this expression using relation 9.131(2) of Ref. [31] that expresses a hypergeometric function of the variable z in terms of hypergeometric functions of the variable $1-z$. For S real we have the following:

$$\begin{aligned}\frac{\Lambda_l(iS)}{\cos\nu}=1+(-1)^l\sin^l\nu\Bigg[&\left|\frac{\Gamma\left(\frac{l+1+iS}{2}\right)}{\Gamma\left(1+\frac{l+iS}{2}\right)}\right|^2\frac{1}{2\cos\nu}\\ &\times{}_2F_1\left(\frac{l+1+iS}{2},\frac{l+1-iS}{2},\frac{1}{2};\cos^2\nu\right)\\ &-{}_2F_1\left(1+\frac{l+iS}{2},1+\frac{l-iS}{2},\frac{3}{2};\cos^2\nu\right)\Bigg].\end{aligned} \tag{D1}$$

For a fixed value of S_l, and, thus, considering α as a function of S_l, we expect the asymptotic expansion in the large l limit:

$$\cos\nu=\frac{a_1}{l}+\frac{a_2}{l^2}+\frac{a_3}{l^3}+\cdots. \tag{D2}$$

Using (D1) for fixed S, the calculation of the leading coefficient a_1 is straightforward, expressing each ${}_2F_1$ function in terms of its defining hypergeometric series, see relation (9.100) in Ref. [31], and taking the large l limit in each term of the series. For example, for any natural integer k,

$$\frac{\left(\frac{l+1}{2}\right)^2\cdots\left(\frac{l+1}{2}+k-1\right)^2}{\left(\frac{1}{2}\right)\cdots\left(\frac{1}{2}+k-1\right)}\frac{\cos^{2k}\nu}{k!}\underset{l\to+\infty}{\to}\frac{a_1^{2k}}{(2k)!}, \tag{D3}$$

$$\frac{\left(\frac{l+2}{2}\right)^2\cdots\left(\frac{l+2}{2}+k-1\right)^2}{\left(\frac{3}{2}\right)\cdots\left(\frac{3}{2}+k-1\right)}\frac{\cos^{2k}\nu}{k!}\underset{l\to+\infty}{\to}\frac{a_1^{2k}}{(2k+1)!}. \tag{D4}$$

The sum over k then generates cosh and sinh functions of a_1. Also, the Γ functions in Eq. (D1) may be expanded using relation 8.344 in Ref. [31]. This lowest-order calculation gives $\Lambda_l(iS_l)/\cos\nu=1-\exp(-a_1)/a_1+O(1/l)$. Since $\Lambda_l(iS_l)$ vanishes (to all orders), one obtains $a_1=\exp(-a_1)$ so

$$a_1=C, \tag{D5}$$

where C was introduced in Eq. (75) in the Born-Oppenheimer context. This technique can be pushed, in principle, to any order. We calculated $a_2=-C/2$ and a_3. That S_l does not contribute to a_2 (and contributes to a_3 in the form of a term S_l^2) is due to the fact that Eq. (D1) is an even function of S and it is always the ratio S/l that appears in the expansion. Turning the expansion [Eq. (D2)] into an expansion for the mass ratio, we obtain Eqs. (78), (79), and (80).

This large-l expansion technique can even be extended to the case where $S_l/l = O(1)$ (which includes both the previous case of S_l fixed and the new case S_l/l fixed). To leading order, one finds $S_l^2 \simeq (\alpha - \alpha_c^{(l)})C^2/2$ (as in the Born-Oppenheimer approximation) and

$$\frac{\Lambda_l(iS)}{\cos\nu} \simeq 1 - \frac{\exp\left[-C\left(\frac{S^2+l^2}{S_l^2+l^2}\right)^{1/2}\right]}{C\left(\frac{S^2+l^2}{S_l^2+l^2}\right)^{1/2}}. \tag{D6}$$

This shows that $\Lambda_l(iS)$ is a function of S of width $\propto l$ in the large l limit, so the derivatives in Eq. (87) tend to zero in that limit and the contribution is dominated by the integral over S. Setting $x_l \equiv S_l/l$, assumed to be bounded as we noted, we then obtain an asymptotic expression for the global scale of the Efimovian spectrum as follows:

$$\begin{aligned}\ln\left(q_{\rm global}^{(l)} R_*/2\right) \underset{l\to+\infty}{=} & \frac{\mathrm{Im}\,[\ln\Gamma(1+iS_l)+\ln\Gamma(1+2iS_l)]}{S_l} \\ & - 3\ln l - \frac{1}{2}\ln\left(1+x_l^2\right)+1 \\ & - \frac{\arctan x_l}{x_l} + \int_0^{x_l}\frac{dx}{x_l}\ln\mathcal{F}(x) \\ & + O\left(\frac{1}{l}\right)\end{aligned} \tag{D7}$$

with the function

$$\mathcal{F}(x) \equiv \frac{1}{x_l^2 - x^2}\left[-1 + \frac{e^{-C\left(\frac{1+x^2}{1+x_l^2}\right)^{1/2}}}{C\left(\frac{1+x^2}{1+x_l^2}\right)^{1/2}}\right]. \tag{D8}$$

In the case where S_l has a fixed value for $l \to +\infty$, one has that $x_l \to 0$ and one may approximate $\mathcal{F}$ by keeping terms up to order x_l^2 and x^2 inside the square brackets of Eq. (D8), so $\mathcal{F}(x) = (1+C)/2 + o(1)$. This gives Eq. (90). In the case where x_l is fixed to a nonzero value, S_l diverges for $l \to +\infty$ so the Γ functions in Eq. (D7) may be Stirling expanded, leading to

$$\begin{aligned}\ln(q_{\rm global}^{(l)} R_*/2) \underset{l\to+\infty}{\overset{x_l\ \text{fixed}}{\to}} & \ln\frac{x_l}{(1+x_l^2)^{1/2}} - \frac{\arctan x_l}{x_l} \\ & + \int_0^{x_l}\frac{dx}{x_l}\ln\left[\left(x_l^2-x^2\right)\mathcal{F}(x)\right].\end{aligned} \tag{D9}$$

Furthermore, if $x_l \gg 1$, the first two terms in the right-hand side of Eq. (D9) tend to zero, and the integral can be shown to approach $J + \ln(1+C)$, where J is the integral [Eq. (92)]. Remarkably, one then recovers for $q_{\rm global}^{(l)} R_*$ the same estimate as in Eq. (91), which was obtained with a different limiting procedure ($S_l \to +\infty$ for l fixed). This may be not surprising, since $S_l/l \gg 1$ in both cases, and this is obvious even in a semiclassical picture, see the discussion below Eq. (107), where the large α limit is reached for $\alpha C^2/2 \gg (l+1/2)^2$ (which implies $S_l \gg l$), irrespective of whether l is large.

APPENDIX E: EFIMOVIAN SPECTRUM GLOBAL SCALE AT INFINITE MASS RATIO

The results [Eqs. (C9) or (87)] are quite useful to determine $q_{\rm global}^{(l)}$ for $\alpha \to +\infty$ for a fixed angular momentum l. One simply needs an asymptotic expansion of $\Lambda_l(iS)$ for S large of the order of $S_l \to +\infty$, which implies that S and $1/\cos\nu$ both scale as $\alpha^{1/2}$. For $S \to +\infty$ it is apparent that the integral over θ in Eq. (41) is dominated by the contribution of a small interval ending in $\theta = \nu$, since here $s = iS$. Approximating $\sin(s\theta)/\sin(s\pi/2) \sim \exp[S(\theta - \pi/2)]$, we see that the small interval has a width scaling as $1/S$. We then Taylor-expand $P_l(\sin\theta/\sin\nu)$ around $\theta = \nu$ up to second order in $(\theta - \nu)$, and we perform the integral over θ extending the lower bound of the integral to $-\infty$, which generates an expansion in powers of $1/S$. We can also consistently expand $\cos\nu$ and $\sin\nu$ up to second order in $\pi/2 - \nu$, since $1/S$ and $\pi/2 - \nu$ are of the same order. If one sets $\epsilon = \pi/2 - \nu$, this gives

$$\begin{aligned}\frac{\Lambda_l(iS)}{\cos\nu} = 1 - \frac{e^{-\epsilon S}}{\epsilon S}\bigg[& 1 + \frac{2}{3}\epsilon^2 - \frac{1}{2}l(l+1) \\ & \times\left(\frac{\epsilon}{S} + \frac{1}{S^2}\right) + O\left(\frac{1}{S^4}\right)\bigg],\end{aligned} \tag{E1}$$

where we used $P_l(1) = 1$ and $P_l'(1) = l(l+1)/2$.

A first application of Eq. (E1) is an expansion of S_l in powers of ϵ. Since $\Lambda_l(iS_l) = 0$, one finds to leading order $S_l\epsilon = C$, where C is given by Eq. (75). Going to next order gives a correction of order ϵ^2 to ϵS_l. Expressing ϵ as a power series in $1/\alpha$ from $\cos\epsilon = \alpha/(1+\alpha)$ gives Eq. (81).

A second application of Eq. (E1) is the derivation of the infinite-mass-ratio limit of $q_{\rm global}^{(l)}$. To leading order, $\Lambda_l(iS)/\cos\nu$ is a function of ϵS and so is

$$R_l(S) \simeq \ln\left[\left(1 - \frac{e^{-x}}{x}\right)\frac{x^2}{x^2 - C^2}\right]\bigg|_{x=\epsilon S}. \tag{E2}$$

This means that the $(2k-1)^{\rm th}$ derivatives of R_l in Eq. (C8) scale as ϵ^{2k-1} and are negligible. The integral over S' in Eq. (C8) is a leading contribution that scales as S_l as revealed by the change of variable $x = \epsilon S'$. Moreover, the denominator in Eq. (C9) contributes with a phase factor $\sim\exp(2iS_l\ln 2)$. Using Eq. (86) one finally obtains Eq. (92).

APPENDIX F: FIRST CORRECTION TO THE HYDROGENOID SPECTRUM

Within the Born-Oppenheimer framework of Sec. IV C, for the hydrogenoid part of the trimer spectrum, we apply the first-order perturbation theory to the $1/r_{23}^{1/2}$ term of Eq. (101) that we call here δV. In terms of the Bohr radius $a_0 = \hbar^2/(m_e e^2) = 4R_*/\alpha$, the normalized hydrogenoid wave function is [64]

$$\begin{aligned}\psi_n^{(l)}(\mathbf{r}_{23}) & \\ = & \left(\frac{2}{(n+l)a_0}\right)^{3/2}\left[\frac{(n-1)!}{2(n+l)(n+2l)!}\right]^{1/2} \\ & \times e^{-r_{23}/[(n+l)a_0]}\left[\frac{2r_{23}}{(n+l)a_0}\right]^l L_{n-1}^{2l+1}\left[\frac{2r_{23}}{(n+l)a_0}\right]Y_l^{m_l}(\mathbf{r}_{23}),\end{aligned} \tag{F1}$$

where L_n^β is the usual Laguerre polynomial defined with the convention of Ref. [31] (and not with the one of Ref. [64]). After angular integration and the change of variable $u = 2r_{23}/[(n+l)a_0]$, we obtain for the expectation value of δV in that wave function

$$\langle \delta V\rangle = \frac{\hbar^2\alpha^{1/2}}{MR_*^2}\frac{(n-1)!}{[2(n+l)]^{3/2}(n+2l)!} \times \int_0^{+\infty} du\, u^{2l+3/2}e^{-u}\big[L_{n-1}^{2l+1}(u)\big]^2. \quad \text{(F2)}$$

To evaluate this integral, we use the generating function technique of Ref. [64]: We define

$$I(x,y) = \int_0^{+\infty} du\, u^{\beta+\gamma}e^{-u}\varphi_\beta(u,x)\varphi_\beta(u,y), \quad \text{(F3)}$$

where eventually we shall set $\gamma = 1/2$ and $\beta = 2l+1$, and where the generating function of the Laguerre polynomials L_n^β for fixed β is given for $|z|<1$ by relation 8.975(1) in Ref. [31]:

$$\varphi_\beta(u,z) \equiv \sum_{n=0}^{+\infty} L_n^\beta(u)z^n = \frac{e^{-uz/(1-z)}}{(1-z)^{\beta+1}}. \quad \text{(F4)}$$

On the one hand, since φ_β is the generating function,

$$I(x,y) = \sum_{m,n=0}^{+\infty} x^m y^n \int_0^{+\infty} du\, u^{\beta+\gamma}e^{-u}L_m^\beta(u)L_n^\beta(u) \quad \text{(F5)}$$

so we need the diagonal terms $n=m$ in this series expansion. On the other hand, from the explicit form of φ_β,

$$I(x,y) = \Gamma(1+\beta+\gamma)\frac{[(1-x)(1-y)]^\gamma}{(1-xy)^{1+\beta+\gamma}}, \quad \text{(F6)}$$

it remains to expand, in a series of x and y using $(1-X)^\nu = \sum_{q=0}^{+\infty} X^q\Gamma(q-\nu)/[\Gamma(q+1)\Gamma(-\nu)]$, where ν is a noninteger, 3 times to obtain, for a noninteger γ,

$$\int_0^{+\infty} du\, u^{\beta+\gamma}e^{-u}\big[L_{n-1}^\beta(u)\big]^2 = \sum_{k=0}^{n-1}\left(\frac{\Gamma(k-\gamma)}{\Gamma(k+1)\Gamma(-\gamma)}\right)^2\frac{\Gamma(\beta+\gamma+n-k)}{\Gamma(n-k)}. \quad \text{(F7)}$$

For $\gamma = 1/2, \beta = 2l+1$, expressing the Γ function of integers and half-integers in terms of factorials finally gives Eqs. (103) and (104) [65].

[1] E. Braaten and H.-W. Hammer, Phys. Rep. **428**, 259 (2006).

[2] J. M. Vogels, C. C. Tsai, R. S. Freeland, S. J. J. M. F. Kokkelmans, B. J. Verhaar, and D. J. Heinzen, Phys. Rev. A **56**, R1067 (1997); E. Timmermans, P. Tommasini, M. Hussein, and A. Kerman, Phys. Rep. **315**, 199 (1999); C. Chin, R. Grimm, P. Julienne, and E. Tiesinga, Rev. Mod. Phys. **82**, 1225 (2010).

[3] T. Kraemer *et al.*, Nature **440**, 315 (2006); M. Zaccanti, B. Deissler, C. D'Errico, M. Fattori, M. Jona-Lasinio, S. Müller, G. Roati, M. Inguscio, and G. Modugno, Nat. Phys. **5**, 586 (2009); N. Gross, Z. Shotan, S. Kokkelmans, and L. Khaykovich, Phys. Rev. Lett. **103**, 163202 (2009); **105**, 103203 (2010); S. E. Pollack, D. Dries, and R. G. Hulet, Science **326**, 1683 (2009); T. Lompe, T. B. Ottenstein, F. Serwane, A. N. Wenz, G. Zürn, and S. Jochim, *ibid.* **330**, 940 (2010); N. Gross, Z. Shotan, O. Machtey, S. Kokkelmans, and L. Khaykovich, C. R. Phys. **12**, 4 (2011).

[4] V. Efimov, Sov. J. Nucl. Phys. **12**, 589 (1971); Nucl. Phys. A **210**, 157 (1973); A. Bulgac and V. Efimov, Sov. J. Nucl. Phys. **22**, 296 (1975).

[5] D. Petrov, Phys. Rev. A **67**, 010703 (2003).

[6] F. Werner, L. Tarruell, and Y. Castin, Eur. Phys. J. B. **68**, 401 (2009).

[7] D. S. Petrov, Phys. Rev. Lett. **93**, 143201 (2004).

[8] J. Levinsen and D. S. Petrov, e-print arXiv:1101.5979 (2011).

[9] E. Wille *et al.*, Phys. Rev. Lett. **100**, 053201 (2008).

[10] T. G. Tiecke, M. R. Goosen, A. Ludewig, S. D. Gensemer, S. Kraft, S. J. J. M. F. Kokkelmans, and J. T. M. Walraven, Phys. Rev. Lett. **104**, 053202 (2010).

[11] A. Gogolin, C. Mora, and R. Egger, Phys. Rev. Lett. **100**, 140404 (2008).

[12] C. Mora, A. Gogolin, and R. Egger, C. R. Phys. **12**, 27 (2011).

[13] G. V. Skorniakov and K. A. Ter-Martirosian, Zh. Eksp. Teor. Phys. **31**, 775 (1956) [Sov. Phys. JETP **4**, 648 (1957)].

[14] M. Holland, S. J. J. M. F. Kokkelmans, M. L. Chiofalo, and R. Walser, Phys. Rev. Lett. **87**, 120406 (2001); J. N. Milstein, S. J. J. M. F. Kokkelmans, and M. J. Holland, Phys. Rev. A **66**, 043604 (2002).

[15] K. Góral, T. Köhler, S. A. Gardiner, E. Tiesinga, and P. S. Julienne, J. Phys. B **37**, 3457 (2004); M. H. Szymańska, K. Góral, T. Köhler, and K. Burnett, Phys. Rev. A **72**, 013610 (2005).

[16] T. Köhler, K. Góral, and P. Julienne, Rev. Mod. Phys. **78**, 1311 (2006).

[17] M. Lee, T. Köhler, and P. Julienne, Phys. Rev. A **76**, 012720 (2007).

[18] V. Gurarie and L. Radzihovsky, Ann. Phys. **322**, 2 (2007).

[19] M. Jona-Lasinio, L. Pricoupenko, and Y. Castin, Phys. Rev. A **77**, 043611 (2008).

[20] B. Marcelis, B. Verhaar, and S. Kokkelmans, Phys. Rev. Lett. **100**, 153201 (2008).

[21] C. Mora, Y. Castin, and L. Pricoupenko, C. R. Phys. **12**, 71 (2011).

[22] Physically this is clear in a real-space reasoning, since it turns the scattered wave $\propto e^{ikr}/r$ into an exponentially decreasing function.

[23] Wu-Ki Tung, in *Group Theory in Physics* (World Scientific, Singapore, 1985).

[24] J. H. Macek, S. Ovchinnikov, and G. Gasaneo, Phys. Rev. A **72**, 032709 (2005); **73**, 032704 (2006).

[25] K. Helfrich, H.-W. Hammer, and D. S. Petrov, Phys. Rev. A **81**, 042715 (2010).

[26] E. Wigner, Zeits. Physik **83**, 253 (1933); H. Bethe and R. Peierls, Proc. R. Soc. London, Ser. A **148**, 146 (1935); S. Albeverio, F. Gesztesy, R. Hoegh-Krohn, and H. Holden, *Solvable Models in Quantum Mechanics* (Springer-Verlag, Berlin, 1988); Y. Castin, *Coherent Atomic Matter Waves*, Lecture Notes of Les

Houches Summer School, edited by R. Kaiser, C. Westbrook, and F. David (EDP Sciences and Springer-Verlag, 2001), p. 1.; Y. Castin, C. R. Phys. **5**, 407 (2004); L. Pricoupenko and Y. Castin, J. Phys. A **40**, 12863 (2007).

[27] F. Werner and Y. Castin, Phys. Rev. A **74**, 053604 (2006).

[28] G. S. Danilov, Sov. Phys. JETP **13**, 349 (1961).

[29] Y. Castin and F. Werner, in *The BCS-BEC Crossover and the Unitary Fermi Gas*, Lecture Notes in Physics, edited by W. Zwerger (Springer, Berlin, 2011), chap. 5.

[30] F. Werner and Y. Castin, Phys. Rev. Lett. **97**, 150401 (2006).

[31] I. S. Gradshteyn and I. M. Ryzhik, in *Tables of Integrals, Series, and Products*, 5th ed., edited by A. Jeffrey (Academic Press, San Diego, 1994).

[32] G. Gasaneo and J. H. Macek, J. Phys. B **35**, 2239 (2002); M. Birse, J. Phys. A **39**, L49 (2006).

[33] Seth T. Rittenhouse, N. P. Mehta, and Chris H. Greene, Phys. Rev. A **82**, 022706 (2010).

[34] Y. Castin and F. Werner, Phys. Rev. A **83**, 063614 (2011).

[35] One uses relation 9.132(1) in Ref. [31] to map the hypergeometric function for a large and negative argument $-k^2/Q^2$ to hypergeometric functions of small and positive argument $Q^2/(Q^2+k^2)$. Second, the product of Γ factors is simplified using the doubling formula 8.335(1) of Ref. [31] as $\Gamma(s) = 2^{s-1}\Gamma(s/2)\Gamma[(1+s)/2]/\sqrt{\pi}$, and then repeatedly the relation $\Gamma(z+1) = z\Gamma(z)$; and, finally, the relation 8.332(2) of Ref. [31] in the form $|\Gamma[(1+s)/2]^2| = \pi/\cos(\pi s/2)$.

[36] The notation $\int_{-\infty+z_0}^{+\infty+z_0} dz$ denotes integration in the complex plane from left to right on the horizontal straight line passing through the complex number z_0.

[37] See, e.g., C. Cohen-Tannoudji, J. Dupont-Roc, and G. Grynberg, in *Atom-Photon Interaction: Basic Process and Applications* (Wiley-VCH, Berlin, 1998).

[38] Our function C_l corresponds to the function C_+ in Ref. [12], up to a Wick rotation, since a Barnes contour integral is used in Ref. [12] rather than the more common Fourier representation.

[39] Under inspection of Eq. (41), one finds that the poles of $S \to \Lambda_l(iS)$, here l odd, necessarily obey $\sin(s\pi/2) = 0$, imposing that s is an even integer. In addition, $s = 0$ is not a pole due to the presence of the factor $\sin(s\theta)$ in the numerator of the integrand in Eq. (41). Moreover, $0 < s < l$ cannot be a pole: According to relation 1.391(1) in Ref. [31], for an s even integer, $\sin(s\theta) = \cos\theta\, Q_s(\sin\theta)$, where $Q_s(X)$ is an odd polynomial of degree $s-1$. Injecting this form into Eq. (41), making the change of variable $u = \sin\theta/\sin\nu$, and using the fact that $P_l(u)$ and $Q_s(u\sin\nu)$ are odd functions of u, one obtains the scalar product between two polynomials, $\int_{-1}^{1} du\, P_l(u) Q_s(u\sin\nu)$. As the Legendre polynomials form an orthogonal basis for this scalar product, the integral vanishes if the degree of Q_s is less than the degree of P_l, that is, $s-1 < l$. Numerically, we have found that the function $s \to \Lambda_l(s)$ is negative for $s = 0$ (here $\alpha > \alpha_c^{(l)}$) and is a decreasing function of s over the interval $[0,l+1[$. So the imaginary roots of $S \to \Lambda_l(iS)$, that is, the real roots of $\Lambda_l(s)$, are obtained by looking for changes of sign of the function $s \to \Lambda_l(s)$ with small steps (typically 100 steps) over each interval of s between the two successive even integers $2n+l+1$ and $2(n+1)+l+1$, $n \geqslant 0$. A dichotomic search is then applied in case of a sign change. The infinite products in Eqs. (70) and (71) are approximated by keeping a maximal value of n, for example, $n = 1000$, leading to exactly the same number of factors in the numerator and in the denominator. A check is to verify that this truncated product in Eq. (70) accurately reconstructs the function $\Lambda_l(iS)/\cos\nu$ over, e.g., the interval $-5 < S < 5$ for $S_l \lesssim 1$, that is, with an error of less than 10^{-5}, otherwise the maximal value of n is increased (we went up to $n = 2500$). We have also used the more rapidly convergent representation [Eqs. (C3) and (C5)].

[40] We recall that the poles of $\Gamma(z)$ are the nonpositive integers $n = 0, -1, -2, \ldots$, that is, $n \in \mathbb{Z}^-$, with residues $(-1)^n/n!$. As a particular consequence, the factor $\Gamma(1+iS+iS_l)$ in the denominator of Eq. (71) leads to the fact that $C_l(S)$ vanishes for $S \to -S_l + ip$ for any integer $p \geqslant 1$, so $\tilde{F}^{(l)}(S)$ has no pole there despite the division by the hyperbolic sine in Eq. (68). Also, according to relation 8.326(1) in Ref. [31], $|\Gamma(x)/\Gamma(x-iy)|^2 = \prod_{k=0}^{+\infty}(1+\frac{y^2}{(x+k)^2})$, for all $x \in \mathbb{R}\setminus\mathbb{Z}^-$ and $\forall y \in \mathbb{R}$, the function $\Gamma(z)$ has no root in the complex plane.

[41] The same work can be gone for $x \to +\infty$. Closing the integration contour by a half-circle at infinity in the upper half of the complex plane, one finds that the leading contribution to $F^{(l)}(x)$ originates from the pole $z = v_0 + i = (l+2)i$ (see Fig. 1) so $D(\mathbf{k})$ vanishes as $1/k^{4+l}$ for $k \to +\infty$.

[42] One splits the functions C_l and Λ_l as $C_l(S) = \frac{\Gamma(iS_l - iS)}{\Gamma(1+iS+iS_l)} C_l^{\text{other}}(S)$ and $\Lambda_l(iS) = \cos\nu(S^2 - S_l^2)\times\Lambda_l^{\text{other}}(iS)$. From $\Gamma(z+1) = z\Gamma(z)$ one then has $C_l^{\text{other}}(S+i) = \Lambda_l^{\text{other}}(iS) C_l^{\text{other}}(S)$ for all real S. A Weierstrass form for $C_l^{\text{other}}(S)$ is deduced from Eq. (71). The property $[\Gamma(z)]^* = \Gamma(z^*)$ and the fact that u_n and v_n are purely imaginary for $n > 0$ then lead to $[C_l^{\text{other}}(z)]^* = C_l^{\text{other}}(-z^*)$ in the complex plane. As a consequence,

$$\left[C_l^{\text{other}}(S_l)\right]^* = C_l^{\text{other}}(-S_l).$$

Expressing C_l^{other} in that equation in terms of the original function C_l (this requires taking a limit $S \to S_l$), together with the relation $|\Gamma(2iS_l)|^2 = \pi/[2S_l\sinh(2\pi S_l)]$, cf. relation 8.332(1) of Ref. [31], gives Eq. (72). Similarly one has $[\tilde{F}^{(l)}(S)]^* = -\tilde{F}^{(l)}(-S^*)$ and $f^{(l)}(k)$ is purely imaginary (for real k).

[43] This can also be obtained from the fact that $\mathcal{A}(\mathbf{x})$ in Eq. (46) scales as $x^{-1\pm s}$ for $x \to 0$ and that the correctly normalized extra-particle wave function (97) involves a factor $\kappa^{1/2} \propto 1/r_{23}^{1/2}$.

[44] O. I. Kartavtsev and A. V. Malykh, Zh. Eksp. Teor. Phys. **86**, 713 (2007).

[45] To efficiently obtain Eq. (80) we took $1/L = 1/(l+1/2)$ as the small parameter, so $\cos\nu = (C/L)[1+\epsilon/L^2 + O(1/L^3)]$ at the critical mass ratio. To calculate sums of the type $S = \sum_{k\geqslant 0} P(k) C^{2k}/(2k)!$, where $P(k)$ is a polynomial, we expanded $P(k) = \sum_{n\geqslant 0} c_n Q_n(k)$ on the basis of polynomials $Q_n(k) = (2k)(2k-1)\ldots(2k-n+1)$. $Q_n(p/2) = 0$ if and only if $0 \leqslant p < n$, p integer, so the coefficients c_n are straightforward to express in terms of the $P(p/2)$'s, and then $S = \sum_{n \text{ even}} c_n C^n \cosh C + \sum_{n \text{ odd}} c_n C^n \sinh C$. For $S = \sum_{k\geqslant 0} P(k) C^{2k+1}/(2k+1)!$, we defined $Q_n(k) = (2k+1)\ldots(2k+1-n+1)$, with $Q_n[(p-1)/2] = 0$ if and only if $0 \leqslant p < n$, p integer, so $S = \sum_{n \text{ even}} c_n C^n \sinh C + \sum_{n \text{ odd}} c_n C^n \cosh C$.

[46] The proportionality of Eqs. (53) and (73) implies that $C_1 k^{iS_l} + \text{c.c.} = \lambda \times (C_2 k^{iS_l} + \text{c.c.})$, where C_1 (respectively, C_2) is the coefficient of k^{iS_l} in the expression between curly brackets in Eq. (53) [respectively, in Eq. (73)] and λ is the proportionality factor. Since the functions $k \to k^{\pm iS_l}$ are linearly independent,

this is satisfied if and only if $C_1 = \lambda C_2$ and $C_1^* = \lambda C_2^*$, that is, $C_1^* C_2/(C_1 C_2^*) = 1$. This last equation may be naturally written is the form $X^{2iS_l} = 1$, which implies that the quantity X is an integer power of $e^{-\pi/S_l}$.

[47] V. Efimov, Phys. Rev. C **47**, 1876 (1993); L. Pricoupenko, Phys. Rev. A **73**, 012701 (2006).

[48] $x \to e^{-x}/x$ indeed decreases from $+\infty$ to 0 for $x \in \mathbb{R}^+$.

[49] For the zero-range limit $b \to 0$ taken in Sec. II to be physically valid, $q_n^{(l)} b$ has to remain smaller than unity.

[50] Note that the difference between the extra-particle mass M and the reduced mass μ does not enter yet at this order.

[51] A. B. Migdal, in *Qualitative Methods in Quantum Theory* (W. A. Benjamin, Boston, MA, 1977).

[52] Starting from Eq. (93), one sets $\psi(\mathbf{r}) = Y_l^{m_l}(\mathbf{r}) f(r)/r^{1/2}$ so $f(r)$ obeys a 2D Schrödinger's equation. One then sets $f(r) = F(x)$ with $x = \ln(r/R_*)$ so $f''(r) + f'(r)/r = F''(x)/r^2$. After multiplication by r^2 one obtains $-F''(x) + W(x)F(x) = 0$, to which one applies the usual WKB approximation. Here $W(x) = (l + 1/2)^2 + R_*^2 e^{2x}[\mathcal{Q}^2 - \alpha\kappa^2(R_* e^x)/2]$, where the r dependence of $\kappa(r)$ is included in the writing. The WKB approximation requires that $|\frac{d}{dx}[|W(x)|^{-1/2}]| \ll 1$ away from the turning points. For $(\mathcal{Q}R_*)^2 e^{2x} \lesssim |s_{\rm BO}^2|$, where $|s_{\rm BO}|$ is given by Eq. (76), this imposes $|s_{\rm BO}| \gg 1$; that is one has to be far from the Efimovian threshold.

[53] Taking the large x_l limit in Eq. (D9) up to and including order $1/x_l$, we obtain exactly Eq. (108), knowing that S_l and $|s_{\rm BO}|$ may be identified at this order. This at least shows that the coefficient of the $1/|s_{\rm BO}|$ term in Eq. (108) is exact in the large l limit. Furthermore, one can extend the estimates (E1) and (E2) to the interval $0 < S \ll 1/\epsilon$ by approximating $\Lambda_l(iS)$ by the limit $\Lambda_l^{\rm app}(iS)$ of Eq. (41) for $\nu \to \pi/2$. Since $-S\Lambda_l^{\rm app}(iS) = \coth(\pi S/2)\prod_{n=0}^{(l-1)/2}\frac{S^2+(2n)^2}{S^2+(2n+1)^2}$, $\int_0^{+\infty} dS \ln[-S\Lambda_l^{\rm app}(iS)] = -(l+1/2)\pi/2$, and one finds from Eq. (87) that Eq. (108) is exact for all l.

[54] S. Gandolfi and J. Carlson, e-print arXiv:1006.5186.

[55] D. Blume and K. M. Daily, Phys. Rev. Lett. **105**, 170403 (2010).

[56] Y. Nishida, D. T. Son, and S. Tan, Phys. Rev. Lett. **100**, 090405 (2008).

[57] O. I. Kartavtsev and A. V. Malykh, J. Phys. B **40**, 1429 (2007).

[58] From the expression of $\check{q}_{\rm rel}(\check{k})$, it is apparent that the actual condition is $qR_*\check{k}_{\max}\cos\nu \gg 1$.

[59] To evaluate in a numerically stable way the integral over u in Eq. (114), we used the fact that $\int_{-1}^{1}\frac{du}{2}P_l(u)/(v-u) = Q_l(v)$, where $v > 1$ and $Q_l(v)$ is a Legendre function of the second kind; see relation 7.224 in Ref. [31]. We then used an open FORTRAN library to calculate that function, see, e.g., mlqnb.f90 in specfun, and also a home-made routine using a high-order $1/v$ expansion, with similar results. Furthermore, for $x \gg 1$ and $X \gg 1$, one has $v \simeq \cosh(x - X)/\sin\nu$, so one faces the function $y \to Q_l[\cosh y/\sin\nu]$, which behaves for $|y| \ll 1$ and for $|\nu - \pi/2| \ll 1$ as $\frac{1}{2}\ln[4/(y^2 + \cos^2\nu)]$. We thus checked that our discretization step for x (and X) verifies $dx = d(\ln\check{k}) < \cos\nu$. Note that, from the usual definition $P_l(u) = (2^{-l}/l!)\frac{d^l}{du^l}[(u^2-1)^l]$, one can show (by l integrations by part) that $Q_l(v) > 0$ for $v > 1$ for l of any parity. The kernel in Eq. (114) has, thus, positive matrix elements for l even and negative for l odd.

[60] We estimate here the issue of magnetic field stabilization for a narrow Feshbach resonance such as the one of ^{6}Li-^{40}K. The $1/a = 0$ assumption imposes the filtering $qR_* > 10R_*/|a|$ on our results, as we noted. The finite experimental value of the scattering length is, according to Eq. (12), $a \approx a_{\rm bg}\Delta B/\delta B$, where δB is the experimental control on the magnetic field. For the modest choice $10R_*/|a| = 10^{-1}$, which amounts to restricting our Fig. 6(a) to $qR_* > 10^{-1}$, and taking typical ^{6}Li-^{40}K Feshbach resonance parameters, $R_* \approx 100$ nm, $\Delta B \approx 0.1$ mT, $a_{\rm bg} \approx 3$ nm [8–10], we reach the condition $\delta B \approx 30{\rm nT} = 0.3$ mG, which requires magnetic shielding but remains accessible [66].

[61] L. Pricoupenko, Phys. Rev. A **82**, 043633 (2010).

[62] D. S. Petrov, G. E. Astrakharchik, D. J. Papoular, C. Salomon, and G. V. Shlyapnikov, Phys. Rev. Lett. **99**, 130407 (2007).

[63] M. Arndt, O. Nairz, J. Voss-Andreae, C. Keller, G. van der Zouw, and A. Zeilinger, Nature **401**, 680 (1999).

[64] P. Caldirola, R. Cirelli, and G. Prosperi, in *Introduzione alla fisica teorica* (Utet, Turin, 1982).

[65] The naive calculation of the integral of Eq.(F7) after expansion of the polynomial in terms of the monomials u^q gives a sum of n^2 terms that suffers the sign problem.

[66] F. Reinhard, Ph.D. thesis, University Pierre et Marie Curie, 2009, in *Design and Construction of an Atomic Clock on an Atom Chip*, p. 84, available at [http://tel.archives-ouvertes.fr/tel-00414386/fr/].